Centromere and Telomere Movements during Early Meiotic Prophase of Mouse and Man Are Associated with the Onset of Chromosome Pairing

Harry Scherthan,* Susanne Weich,* Herbert Schwegler,‡ Christa Heyting,§ Michael Härle,‖ and Thomas Cremer¶

*Department of Human Genetics and Human Biology, University of Kaiserslautern, D-67653 Kaiserslautern, Germany; ‡Institute of Anatomy, University of Magdeburg, D-39120 Magdeburg, Germany; §Department of Genetics, University of Wageningen, 6703 HA Wageningen, The Netherlands; ‖Institute of Pathology, Klinikum, D-68135 Mannheim, Germany; and ¶Institute of Anthropology and Human Genetics, Ludwig-Maximilians University of Munich, D-80333 Munich, Germany

Abstract. The preconditions and early steps of meiotic chromosome pairing were studied by fluorescence in situ hybridization (FISH) with chromosome-specific DNA probes to mouse and human testis tissue sections. Premeiotic pairing of homologous chromosomes was not detected in spermatogonia of the two species. FISH with centromere- and telomere-specific DNA probes in combination with immunostaining (IS) of synaptonemal complex (SC) proteins to testis sections of prepuberal mice at days 4–12 post partum was performed to study sequentially the meiotic pairing process. Movements of centromeres and then telomeres to the nuclear envelope, and of telomeres along the nuclear envelope leading to the formation of a chromosomal bouquet were detected during mouse prophase. At the bouquet stage, pairing of a mouse chromosome-8–specific probe was observed. SC-IS and simultaneous telomere FISH revealed that axial element proteins appear as large aggregates in mouse meiocytes when telomeres are attached to the nuclear envelope. Axial element formation initiates during tight telomere clustering and transverse filament–IS indicated the initiation of synapsis during this stage. Comparison of telomere and centromere distribution patterns of mouse and human meiocytes revealed movements of centromeres and then telomeres to the nuclear envelope and subsequent bouquet formation as conserved motifs of the pairing process. Chromosome painting in human spermatogonia revealed compacted, largely mutually exclusive chromosome territories. The territories developed into long, thin threads at the onset of meiotic prophase. Based on these results a unified model of the pairing process is proposed.

PAIRING of homologous chromosomes during meiotic prophase of sexually reproducing organisms culminates in the formation of the synaptonemal complex (SC)[1] (for reviews see von Wettstein et al., 1984; Giroux, 1988). The SC is composed of axial elements (cores) that connect sister chromatids along their entire length. These become lateral elements when they get interconnected by transverse filaments to result in the well-known tripartite SC structure (Schmekel and Daneholt 1995). While chromosome pairing and meiotic recombination can apparently occur without SC formation (Roeder, 1990; Padmore et al., 1991; Hawley and Arbel, 1993; Loidl et al., 1994*a*; Scherthan et al., 1994; Weiner and Kleckner, 1994; Nag et al., 1995), tripartite SC assembly seems to be a prerequisite for proper chiasma distribution (Sym and Roeder, 1994).

In some species, homologous chromosomes (hereafter referred to as homologues) occupy a joint territory before commencement of meiosis (somatic/vegetative pairing). This is the case in Diptera (e.g., Metz, 1916; Wandall and Svendsen, 1985; Hiraoka et al., 1993), in diploid strains of fission yeast (Scherthan et al., 1994), and possibly in budding yeast (Loidl et al., 1994*a*; Weiner and Kleckner, 1994; for a contrary view see Guacci et al., 1994). In the majority of organisms, however, a precondition of synapsis is the prealignment of homologues, i.e., a process that establishes their close proximity and proper orientation during early meiotic prophase (e.g., Zickler, 1977; Rassmusen and Holm, 1980; Albini and Jones, 1987; Scherthan et al., 1992;

Address all correspondence to H. Scherthan, University of Kaiserslautern, P.O. Box 3049, D-67653 Kaiserslautern, Germany. Tel.: 49 631 205 3251. Fax: 49 631 205 2878.

1. *Abbreviations used in this paper*: AEP, axial element protein; DAPI, 4′6-diamidino-2-phenylindole; FISH, fluorescence in situ hybridization; IS, immunostaining; NE, nuclear envelope; pp, post partum; SC synaptonemal complex; TFP, transverse filament protein of the SC; TEM-ISH, transmission electron microscopy in situ hybridization.

Armstrong et al., 1994; Cheng and Gartler, 1994; Dawe et al., 1994). How this process is accomplished and what its general topological prerequisites are is still a matter of debate (e.g., Maguire, 1988; Loidl, 1990; Kleckner and Weiner, 1993; Moens, 1994).

Centromeres (kinetochores; for review see Rickards, 1981) and telomeres (for reviews see Gilson et al., 1993; Ashley, 1994; Blackburn, 1994) have been considered as key structures of meiotic chromosomes. A solid body of cytological investigations indicates that they play an important role in the chromosome pairing process at meiosis (Rhoades, 1961; Rasmussen and Holm, 1980; Fussell, 1987; Dernburg et al., 1995).

Recently, it has been shown that at induction to meiosis, telomeres of *Schizosaccharomyces pombe* chromosomes attach to the spindle pole body (the equivalent of the centrosome of higher eukaryotes) of the parental nuclei and lead chromosome movements that persist throughout karyogamy and the entire meiotic prophase (Chigashige et al., 1994, Svoboda et al., 1995). In diploid *S. pombe* strains homologues occupy joint territories during vegetative growth, while telomere clustering is the first meiosis-specific event at the onset of azygotic meiosis (Scherthan et al., 1994). The resulting bouquet configuration is maintained throughout the entire prophase and is thought to be a prerequisite for meiotic chromosome pairing and the high level of meiotic recombination in this asynaptic organism (for review see Kohli, 1994). Bouquet formation (telomere clustering) seems to be a consistent motif of the pairing process of nearly all eukaryotic species of different kingdoms studied so far (Fussell, 1987; Dernburg et al., 1995). It has been proposed that it "might support the sort out process of homologs prior to their actual pairing" (Therman and Sarto, 1977), but its role in the pairing process has remained enigmatic (see Loidl, 1990).

As we are interested in the preconditions and course of meiotic chromosome pairing, we have undertaken an investigation of the meiotic pairing process in three-dimensionally preserved meiocytes from paraffin testis sections of *Mus musculus.* The mouse was chosen as a model because its spermatogenesis is well-characterized (e.g., Oakberg, 1956; Bellvé et al., 1977*a*,*b*; Oud and Reutlinger, 1981; Dietrich and de Boer, 1983; de Rooij, 1988) and commences in the postnatal mouse fairly synchronously (Bellvé et al., 1977*b*; Kluin and de Rooij, 1981; Goetz et al., 1984; Vergowen et al., 1991). The histological context in combination with fluorescence in situ hybridization (FISH) and immunostaining patterns was exploited to identify meiotic stem cells and meiocytes. FISH experiments with telomeric, centromeric, and chromosome-8–specific subregional DNA probes carried out on prepuberal and adult mouse testis tissue sections (Scherthan and Cremer, 1994) revealed sequential changes of centromere and telomere positions during the onset of meiotic prophase. Immunostaining of SC proteins (Offenberg et al., 1991; Meuwissen et al., 1992, Lammers et al., 1994) in combination with telomere FISH in the same cells showed that telomere movements are associated with the onset of synaptic chromosome pairing.

Human testis tissue sections were also analyzed by FISH with telomere and centromere probes. The results were compared with the mouse data and revealed telomere movements and pre-bouquet centromere movements as conserved topological motifs of the pairing process in the distantly related mammals. Painting of chromosomes 1 revealed rather compact, predominantly separate territories in human spermatogonia. In spermatocytes I these underwent a dramatic change in shape and developed into the well-known, threadlike prophase chromosomes.

Materials and Methods

DNA Probes and Labeling

Mouse chromosome-8–specific, repetitive subsatellite DNA clones (Boyle and Ward, 1992) and a repetitive, chromosome 12–specific subsatellite DNA probe were kind gifts of D.C. Ward (Yale University, New Haven, CT). Human chromosome 1–specific plasmid library (pBS1; Collins et al., 1991) was kindly provided by J.W. Gray, DMC, UC San Francisco, CA. Human chromosome 1–specific subregional probe pUC 1.77 (Cooke and Hindley, 1979) was used to probe for region 1q12.

A 42mer deoxynucleotide oligomere homologous to the pericentromeric mouse major satellite (Scherthan and Cremer, 1994) and a cloned human alpha satellite DNA probe located at all human centromeres (Mitchell et al., 1985) were used as the probes for centromeric heterochromatin in the respective species. $(TTAGGG)_7/(CCCTAA)_7$ oligomeres (Moyzis et al., 1988) were used to illuminate mouse and human telomeres. Specificity of oligomeres was confirmed by FISH to metaphase chromosomes (not shown).

Labeling of oligomeres with biotin-16-dUTP or digoxigenin-11-dUTP (both Boehringer Mannheim, Inc., Mannheim, Germany) by terminal tailing was performed as described (Scherthan and Cremer, 1994). Plasmid DNA was labeled with biotin-14-dATP (Life Technologies, Inc., Gaithersburg, MD) or digoxigenin-11-dUTP (Boehringer Mannheim, Inc.) using a nick translation kit (Life Technologies, Inc.) according to the instructions of the supplier.

Tissue Origin and Processing

Several adult and prepuberal male BALBc mice (d 4, 6, 8, 10, 12 postpartum [pp]) (stocks of the Institute of Anatomy, University of Freiburg, Germany) were killed and transcardially perfused with 4% paraformaldehyde/PBS for 15 min. Testes were removed and embedded in paraffin following standard procedures. Human testis tissue obtained by biopsy was fixed for 4 h in phosphate buffered formaldehyde (4%). Thereafter, tissue was embedded in paraffin, and 8–15-μm sections were cut from paraffin blocks and floated on a clean 37°C water bath. They were picked up with 3-aminotriethoxy-propylsilane–(Merck Darmstadt, Germany) coated slides and air-dried for >30 min at 65°C (for details see Scherthan and Cremer, 1994).

Immunostaining of SC Proteins

Polyclonal antisera against rat lateral element antigens of 30 and 33 kD (Lammers et al., 1994) and transverse filament proteins (SCP1; Meuwissen et al., 1992) of the rat SC were used to stain mouse SC proteins. The appearance of these proteins in rat meiosis is stage specific (Heyting et al., 1988; Dietrich et al., 1992), and the specificity of rat SC antisera to mouse SCs has been demonstrated (Moens et al., 1987). Immunostaining of these proteins in mouse testis paraffin sections was performed in sections deparaffinized in xylene and rehydrated through a decreasing ethanol series. Sections were pepsin digested (Sigma Chemical Co., St. Louis, MO; 100 μg/ml H_2O, pH 2.0) for 30 min at 37°C and postfixed in 1% formaldehyde/PBS for 5 min. After a brief wash in PBS, excess liquid was drained and antibody solution (rabbit anti 30 + 33–kD polyclonal serum diluted 1/50 in PBS, 0.1% Tween 20) was applied. After incubation for 30 min at 37°C and three 3-min washes in PBS, a secondary goat anti–rabbit Cy3–conjugated antibody (Vector Laboratories, Inc. Burlingame, CA; diluted 1/500 in PBS) was added to the preparations. After a final wash in PBS slides were mounted in antifade solution (Vector Laboratories, Inc.). After microphotography, slides were washed in PBS and subjected to FISH without further pretreatment. In some experiments FISH was performed first and hybrid molecules and SC proteins were detected simultaneously with the respective antibodies.

Immunostaining reactions to nonmeiotic cells of mouse tumor cell lines

as well as immunostaining (IS) without the first antibody were performed as negative controls (not shown). Furthermore, nonmeiotic cells (Leydig and Sertoli cells) within testis sections were monitored for background staining.

In Situ Hybridization to Tissue Sections and Probe Detection

Pretreatments as well as fluorescence and electron microscope in situ hybridization to paraffin tissue sections were performed as described in detail by Scherthan and Cremer (1994).

Light Microscopic Evaluation

Preparations were evaluated using an epifluorescence microscope (Axioskop; Carl Zeiss Jena, Inc., Jena, Germany) equipped with single and double band pass filters for excitation of blue and for simultaneous excitation of red and green fluorescence (Chroma Technologies, Brattleboro, VT). Microphotographs were recorded on color slide film (Elite 400; Eastman Kodak Co., Rochester, NY).

Three-dimensional evaluation of hybridized nuclei was performed in most experiments by careful focusing through the nuclei using a 100× plan neofluor lens (for an example see Fig. 7, *c* and *f*). In some cases light optical serial sections were obtained with a confocal laser scanning microscope (Carl Zeiss Jena, Inc.). In the latter case red and green fluorescence was exited with an argon laser at 488 nm and a helium neon laser at 534 nm, respectively.

Transmission Electron Microscopy

After in situ hybridization and HRP/DAB detection tissue sections were embedded in a layer of Epon. This layer was removed from the glass slide by repeated freezing and thawing in liquid nitrogen. Section fragments were reblocked in Epon. Ultrathin sections were cut on an ultratom S (Leica, Inc., Stuttgart, Germany) using a diamond knife and transferred to EM grids. For details see Scherthan and Cremer (1994). Photographs were taken on an electron microscope (EM 10; Carl Zeiss Jena, Inc.).

Results

Identification of Cells in Testis Tissue Sections by Histological Context, FISH, and SC Immunostaining Patterns

In testis tissue sections meiotic stem cells (spermatogonia) were identified by their close association with the tubule membrane. A-type spermatogonia exhibit an elliptical nucleus, while a second category of cells associated with the basement membrane exhibits a more round nucleus. The latter category includes cycling A-type, I-type, B-type, and resting primary spermatocytes before the onset of premeiotic S-phase (early preleptotene) (e.g., de Rooij, 1988; Vergouwen et al., 1993, and references therein). Early preleptotene cells perform premeiotic DNA replication and enter meiotic prophase I. Postreplication preleptotene spermatocytes were classified as mid-preleptotene. They could be identified by their unique centromeric satellite DNA distribution (with sat-DNA compressed to the nuclear envelope) and the occasional appearance of signal doublets with the chromosome-8–specific probe (see below). Late-preleptotene cells were identified by peripheral telomere signal distribution, separate chromosome-8–specific repeats, and the presence of intranuclear axial element protein aggregates (see below). A classical leptotene stage with complete, unpaired axial elements has not been detected in this and earlier investigations on meiotic prophase of the male mouse (e.g., Oud and Reutlinger, 1981; Dietrich and de Boer, 1983; Guitart et al., 1985), thus it is not referred to hereafter.

Zygotene cells are located distant from the basement membrane and were identified by peripheral telomere signals, SC immunostaining, and an increased nuclear diameter. Measurements of nuclear diameters of transverse filament immunostained nuclei from paraffin sections (not shown) revealed that zygotene nuclei exhibited a mean diameter of 9.1 ± 0.6 μm (based on 61 nuclei). Pachytene nuclei are most abundant in testis sections. They were identified by peripheral telomeres and satellite clusters, SC immunostaining (showing a sex vesicle), and a further increase of the nuclear diameter to 12.5 ± 0.86 μm (based on 55 nuclei). The varying numbers of nuclei studied at different stages during earliest meiotic prophase generally reflect the frequency with which these stages were encountered in the tubuli studied. For rare events, e.g., full bouquet stage, more tubuli were scrutinized than for the more abundant stages (e.g., pachytene).

Homologous Chromosome-8 Subsatellite Domains Are Not Aligned in Mouse Spermatogonia

The first set of experiments addressed the question of whether there is a somatic association of homologous chromosomes in spermatogonia of the mouse. To investigate this issue, a mouse chromosome-8–specific subsatellite repeat was hybridized in situ to testis tissue section nuclei of adult mice. Signals generated by FISH with the chromosome-8–specific probe were classified as unpaired when the two signal boundaries were separated by more than the diameter of one signal (>1 μm). Nuclei with signal boundaries separated by less than one signal diameter (<1 μm) but not touching each other were scored as aligned. This category accounts for nuclei with homologous regions in spatial proximity, because contacts of homologue territories outside the illuminated regions go unnoticed. Nuclei with signals that touched each other or had fused into a single, large signal spot were classified as paired, as this signal configuration indicates physical interaction of the chromatin of the illuminated homologous regions.

Two separated signals were observed in 91% of A-type spermatogonia (n = 65), while 9% displayed aligned signals (Table I). Round spermatogonia (spermatogonia developing toward the spermatocyte stage) exhibited separated signals in 86% of cells (n = 79), while 10% displayed aligned signals (Fig. 1; Table I). One signal was observed in three nuclei, possibly representing truncated nuclei (Hopman et al., 1991). Mid-preleptotene nuclei, as identified by their peripheral satellite DNA distribution (see below), displayed separate signals in 96% of cells (n = 25; see Fig. 4 *b*), while 4% exhibited aligned signals (Table I).

High levels of pairing were first detected in zygotene nuclei (n = 68) as identified by axial element protein immunostaining. Paired signals were present in 72% of nuclei, while 28% of nuclei showed aligned signals. Pachytene spermatocytes I displayed paired signals in all nuclei (n = 70) investigated (Table I). Furthermore, a change in signal morphology was observed. Spermatogonia exhibited rather compact, round signals with a mean diameter of 1.0 ± 0.17 μm (n = 45 signals). In mid-preleptotene spermatocytes

Table I. Distribution of Chromosome 8 Subregions in Spermatogonia and Spermatocytes of the Adult Mouse Testis

Cell type	#8 signals	Nuclei	Percent
A-type	Separated	59	91
spermatogonia*	Aligned	6	9
	Fused	0	0
Round	Separated	68	86
Spermatogonia*	Aligned	8	10
	Fused	3	4
Mid-preleptotene	Separated	24	96
spermatocytes‡	Aligned	1	4
	Fused	0	0
Zygotene	Separated	0	0
spermatocytes§	Aligned	19	28
	Fused	49	72
Pachytene	Separated	0	0
spermatocytes§	Aligned	0	0
	Fused	70	100

*Spermatogonia were identified according to their nuclear morphology, satellite DNA distribution, and association with the basement membrane of tubules.
‡Mid-preleptotene nuclei were identified by the peripheral distribution of centromeric satellite DNA.
§Zygotene and pachytene cells were identified by simultaneous immunostaining of axial/lateral element proteins. Aligned represents nuclei where signals were separated by a distance < the signal diameter (for further details see text).

the mean diameter increased to 1.26 ± 0.29 μm (n = 12; analysis was restricted to round signals). In zygotene nuclei signal diameter increased to a mean of 1.49 ± 0.29 μm (n = 29). In pachytene nuclei signals displayed an even more decondensed morphology, often seen as an elongated signal cloud or two signal clouds touching each other (Fig. 1). The latter most likely represent the chromatin loops of the two homologues attached to their common SC core. At their maximum extension signal clouds measured 2.66 ± 0.56 μm (n = 29). One highly compacted signal was generally observed in spermatids (1.0 ± 0.11 μm; n = 35) and sperm heads (0.79 ± 0.21 μm; n = 22) (Fig. 1) reflecting chromatin compaction during spermiogenesis.

To test whether the chromosome-8–specific signal distribution is representative for a general premeiotic chromosome topology, FISH with a mouse chromosome-12–specific subsatellite repeat was performed to testis sections (not shown). Separate signals were present in 84% of spermatogonia analyzed (n = 25), while 12% displayed aligned signals and 2% showed paired signals.

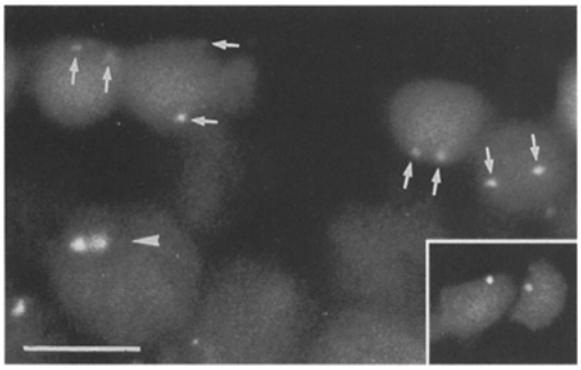

Figure 1. FISH of a subcentromeric chromosome-8 repeat to adult mouse testis sections reveals two separate hybridization signals in several spermatogonia (*arrows*). Pachytene spermatocytes show a single large hybridization signal that consists of two touching signal clouds (*arrowhead*). Inset shows two sperm nuclei with one compacted signal each. Bar, 10 μm.

Chromosome 1 Territorries and Centromeres Are Not Aligned in Human Spermatogonia

To investigate the state of homologue pairing in human meiotic stem cells as well, we delineated chromosome 1 territories by chromosome painting in spermatogonia from human paraffin testis tissue sections (Fig. 2, *a–c*). In a total of 23 well-hybridized spermatogonia, 78% displayed two compact chromosome territories, that were separated by unstained chromatin (Fig. 2 *a*). FISH with a human chromosome-1–specific, subcentromeric (1q12) repeat probe (pUC1.77) showed that out of 96 spermatogonia analyzed 82% displayed separate signals, while 18% showed aligned signals. This signal distribution indicates that homologues in human spermatogonia are predominantly separated. Furthermore, it is apparent that the distribution patterns obtained by FISH with centromere probes reveal comparable results to the ones obtained by chromosome paint probes from the same chromosome, and thus are a good marker for premeiotic chromosome distribution. The chromosome 1 painting analysis furthermore revealed that the compacted chromosome territories seen in spermatogonia (Fig. 2 *a*) had developed into long, cord like territories at leptotene/zygotene, the ends of which seemed to be associated with the nuclear envelope (NE) (Fig. 2 *b*). In pachytene nuclei a single signal tract meandering throughout the nucleus indicated tight pairing of homologues. The painted pachytene chromosomes often displayed a 'chromomere like' pattern (Fig. 2 *c*).

In conclusion, the results obtained in the mouse and the observations made with a repetitive and a chromosome paint probe in human spermatogonia indicate that the behavior of chromosome-specific repeat probes is representative for the general state of homologue distribution. Thus, one can conclude that homologues are variably arranged and predominantly separated in meiotic stem cells, prepuberal spermatogonia, and preleptotene nuclei.

Sequential Order of Meiotic Centromere and Telomere Arrangements and Their Relation to Prealignment Pairing and Synapsis Initiation

The drastic redistribution of chromosome-specific signals leading to their pairing at zygotene/pachytene suggested a fair amount of chromosome movement being associated with the pairing process. Previous investigations have suggested that the redistribution of centromeres and/or telomeres is associated with chromosome pairing at meiosis (e.g., Rickards, 1975; Boiko, 1983; Dawe et al., 1994). Thus, we addressed the question whether these chromosomal domains are involved in the pairing process of the mouse by FISH with centromeric major satellite and telomere-specific probes (Scherthan and Cremer, 1994) to testis sections. The major satellite of the mouse reveals the position of mouse centromeric heterochromatin (except that of the Y chromosome; Pardue and Gall, 1970) at metaphase and interphase. Telomeres of the 40 (2n) acrocentric mouse chromosomes were stained by FISH with $(TTAGGG)_7$ repeat (Moyzis et al., 1988) probes. Unless otherwise stated, the term telomere refers to the signals at

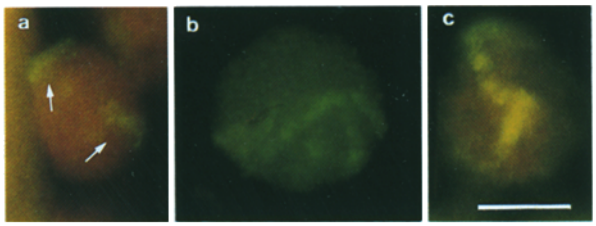

Figure 2. (*a*) Painting of human chromosome 1 in a spermatogonium reveals two separate, compacted territories (*arrows, yellow*). The basement membrane of the testis tubule is located to the left. (*b*) Leptotene nucleus showing elongated, bent-aligned chromosome 1 territories. Ends of territories are apparently at the NE. (*c*) Tightly paired homologues meandering as a single signal tract throughout a pachytene nucleus. The signal tract resembles a 'chromomere like' pattern. The focal plain is at the top of the nucleus. Bar, 5 μm.

distal as well as proximal chromosome ends. The close association of centromeric satellite DNA with the adjacent telomere allows for the identification of proximal telomeres. On a theoretical basis a maximum of 80 individual telomere signals representing the ends of the 40 chromosomes can be expected in the mouse G1 nucleus. For technical reasons, e.g., insufficient saturation of some target regions or truncation of nuclei (Hopman et al., 1991), it can be anticipated that in some nuclei a few signals went undetected by the FISH assay. Thus, the telomere behavior described below characterizes the general behavior of these chromosomal domains during meiotic prophase.

As it is notoriously difficult to derive a sequential order of dynamic events by investigation of cells in fixed material, we performed an analysis in paraffin testis sections of mice at increasing age pp (d 4, 6, 8, 10, and 12 pp). In the prepuberal mouse the onset of spermatogenesis is fairly synchronous (see introduction) and allows for a sequential analysis of the pairing process without drug synchronization methods. Fig. 3 *A* was deduced from the observations described below and may serve as a guide to the emerging

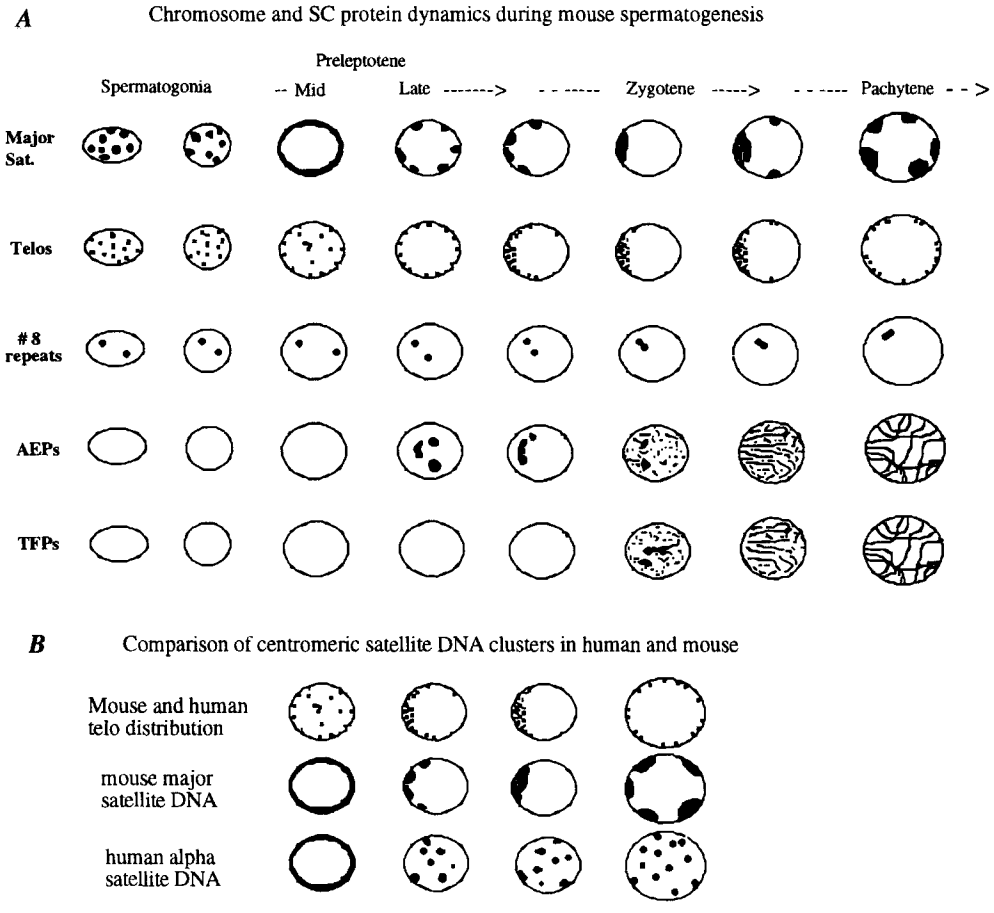

Figure 3. (*A*) Schematic outline of the sequential appearance of distribution patterns of centromeric major satellite DNA (*Major Sat*), telomeres (*Telos*), and chromosome-8–specific subsatellite repeats (*#8 repeats*) in spermatogonia and spermatocytes I of the mouse. The appearance of 30–33-kD axial element proteins (*AEPs*) and transverse filament proteins (*TFPs*) of the SC is depicted in relation to telomere movements and chromosome pairing at prophase. Nuclei within a column exhibit the representative distribution of a probe within a nucleus at a particular developmental stage. The sequence was derived by pairwise or triple combinations of various probes (see Results). In this investigation a classical leptotene stage could not be observed. Therefore, such a stage has not been included in the scheme. Size of nuclei roughly drawn to scale. (*B*) Schematic comparison of prophase rearrangements of centromeric satellite DNA in meiocytes of mouse and man. While telomere distribution in mouse and man is similar during meiotic prophase, centromere distribution is at variance. Human prophase nuclei were identified according to their centromere/telomere distribution patterns as compared to that of mouse spermatogenetic nuclei. It is evident that an equivalent stage to mid-preleptotene nuclei of the mouse (centromeric sat DNA moved to the NE; interior and peripheral telomeres) is present in human prophase. In meiocytes with exclusively peripheral telomeres, mouse centromeric major satellite DNA (due to its physical vicinity to proximal telomeres in acrocentric chromosomes) occupies a peripheral distribution. In human leptotene-pachytene meiocytes telomeres are attached to the NE (compare Rasmussen and Holm, 1978), while α-satellite DNA at centromeres of the predominantly submetacentric chromosomes is generally remote from the NE.

highly dynamic picture of the pairing process. In this scheme each column of nuclei reveals the representative distribution pattern of a particular probe in the respective cell type, as identified by the consecutive appearance in the prepuberal testis. As the crucial steps of the pairing process were observed in individual, fixed meiocytes from testis sections obtained at d 10 pp (late preleptotene, zygotene; see below) the combinatorial use of probes—satellite DNA staining, telomere FISH together with visualization of one of either: chromosome-8 repeats, AEPs, or TFPs in the same cell—was applied to define the sequential order of events. The findings of the various probe combinations are described below. The data of the individual experiments have been compiled in Tables II–IV, which may serve as a guide to the criteria of staging of the individual nuclei. The observed labeling patterns are described below, as if they were observed within a single meiocyte.

In some of the images presented in Fig. 4 and the following figures representative nuclei are shown. It should be noted that FISH signals outside of the nucleus of interest are a consequence of the density of cells encountered in tissue sections. Thus, these have been disregarded in the description of the images. To reveal the outline of 4′6-diamidino-2-phenylindole (DAPI)-counterstained nuclei and to study specific FISH signal patterns, we focused carefully through a large number of nuclei by conventional fluorescence microscopy. In some of the images showing nuclei with clustered telomeres, not all telomere signals are displayed exclusively at the NE as compared with the DAPI image (see e.g., Fig. 5, *e*, *f*, and *h*). In these nuclei, focusing in different planes revealed that some telomere signals were slightly out of focus. They were seen at the nuclear boundary at a somewhat higher or lower focal plane. In this and the following sections we restrict the detailed description to typical nuclei of meiocytes, which can be unequivocally identified in each image.

Transition of Centromeres to the Nuclear Envelope Is the Earliest Detectable Event at the Chromosomal Level

Mouse testis sections at d 4 pp exhibit gonocytes, prepuberal A-type spermatogonia, and immature Sertoli cell nuclei (see Vergouwen et al., 1991). FISH with pericentromeric and telomere-specific DNA probes to these cells showed numerous major satellite clusters and telomere signals at the nuclear periphery as well as dispersed throughout the nuclear interior (n = 50 cells; not shown).

Within tubuli of testis sections obtained at d 6 pp a subset of cells displayed a dramatically changed nuclear topography, i.e., their nuclei conspicuously exhibited most of the centromeric satellite DNA compressed in flakes against the NE as seen by conventional fluorescence microscopy (Fig. 4 *a*) and confocal laser scanning microscopy (Fig. 4 *b*). This satellite distribution is typical of mid-preleptotene (see above) and has been observed in young primary spermatocytes (Oud and Reutlinger, 1981; see Fig. 7 *b*). Occasionally, nuclei with one or two interior satellite DNA clusters were observed. Telomeres were distributed in the nuclear interior as well as at the NE of mid-preleptotene nuclei. Within 10% of these (n = 59), accumulations of a subset of interior, distal telomeres (not adjacent to centromeric satellite DNA) were observed (Fig. 4 *b*). At d 6 pp mid-preleptotene nuclei were detected in a few tubuli of a testis cross section, where they composed 7–22% of cells/tubule (n = 8 tubuli). At d 8 pp they were seen in most tubuli of a testis cross section and represented 9–30% of cells/tubule (n = 11 tubuli).

At d 10 pp a more advanced subset of gonocytes appeared which exhibited centromeric satellite DNA in a few bright staining clusters (2–8; n = 20) at the nuclear periphery, while telomere signals were also seen exclusively at the nuclear periphery. On the basis of these and the experiments described below such nuclei were classified as late-preleptotene.

The findings summarized above are consistent with previous reports that showed that in prepuberal mouse testis at d 8, 9, and 10 pp a substantial fraction of cells is in the preleptotene stage (Bellvé et al., 1977*b*; Goetz et al., 1984). The latter authors found 98% of prophase cells at the preleptotene stage at d 9 pp. The time course observed correlates also with findings on hydroxyurea synchronized spermatogenesis of adult mice (Dietrich and de Boer, 1983).

Homologue Alignment Coincides with Tight Telomere Clustering at the Nuclear Envelope

To investigate further the relation of the observed centromere and telomere movements to homologue pairing, two-color FISH with telomere and a chromosome-8–specific subregional DNA probe in combination with DAPI staining of satellite DNA were performed to testis sections of d 4, 6, 10, and 12 pp mice (Table II). At d 10 and 12 pp all cell types of the spermatogenic line up to zygotene (10 pp) and pachytene (12 pp) are present. Staging of nuclei was achieved by the histological context and the intranuclear position of satellite DNA and telomeres (see above).

In prepuberal gonocyte and spermatogonia nuclei (n = 50) telomere and chromosome-8–specific signals were distributed throughout the nucleoplasm at no obvious order (Fig. 5 *a*). Mid-preleptotene cells (n = 30) showed centromeric satellite DNA pressed to the NE, while probed chromosome-8 regions were predominantly separate (Fig. 5 *b*; Table II). In a subset of these nuclei (23%) the repetitive and presumably late replicating chromosome-8–specific probe produced signal doublets (Fig. 5 *b*), which is indicative for replicated target DNA (Selig et al., 1992). In contrast to somatic G2 nuclei, replicated meiotic chromosomes have their sister chromatids tightly associated, which in the majority of nuclei causes signal spots on sisters to coalesce into a single signal (Scherthan et al., 1994; Weiner and Kleckner, 1994).

At d 10 pp testis cross sections of 31 out of 152 tubuli investigated contained 3–8 early prophase cells (late preleptotene–zygotene), that could be identified by their apparently brighter DAPI staining (4C DNA content), peripheral satellite DNA clusters, and peripheral telomere distribution patterns. Various motifs of telomere clustering with respect to pairing of the chromosome-8 signals (Fig. 5, *c–h*) were observed in these cells (Table II).

Late preleptotene/early zygotene (for staging see Fig. 3 *A* and below) cells showed various degrees of clustering of peripheral telomeres (bouquet formation). In such nuclei

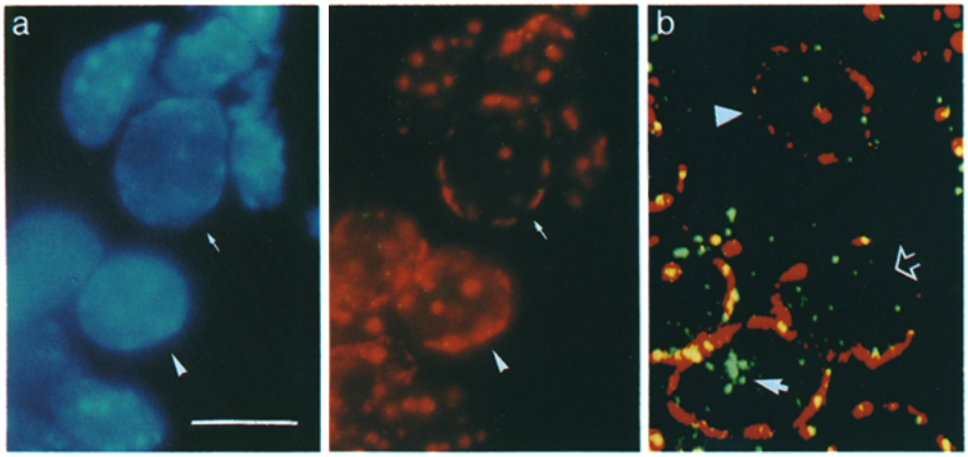

Figure 4. (*a* and *b*) Nuclei of a mouse paraffin testis section obtained at d 6 pp: (*a*) DAPI image (*left*, *blue*) shows nuclei with numerous brightly stained heterochromatin clusters in prepuberal Sertoli cells, primitive spermatogonia, and two mid-preleptotene nuclei (*arrow*, *arrowhead*). (*a*, *right*) Dual band pass image of the same section after two color FISH with major satellite DNA (*red*) and telomere sequences (*yellowish*). Two mid-preleptotene nuclei exhibit numerous satellite DNA clusters at the nuclear periphery. One of them (*arrow*) displays most centromeric satellite DNA compressed against the NE, while an interor satellite cluster is also seen. The other (*arrowhead*) shows peripheral satellite DNA and two more compacted, internal satellite clusters. Telomere signals (*yellow*) are seen at the nuclear periphery and the nuclear lumen as well. Telomere signals were clearly visible in single-bandpass FITC excitation (not shown). (*b*) Light optical section obtained with a CLSM at the maximum nuclear diameter of several other mid-preleptotene nuclei (*arrowhead*, *arrows*). Distal telomeres (*green*) are seen in the nuclear interior while proximal, centromere-associated telomeres are peripheral and colocalize (*yellow signals*) with centromeric satellite DNA (*red*) at the nuclear envelope. One nucleus (*arrowhead*) displays internal telomeres and an internal satellite cluster, while a second nucleus (*open arrow*) shows peripheral satellite DNA and numerous internal distal telomeres. A third nucleus reveals a fraction of distal telomeres associated in the interior (*solid arrow*). Bar, 10 μm.

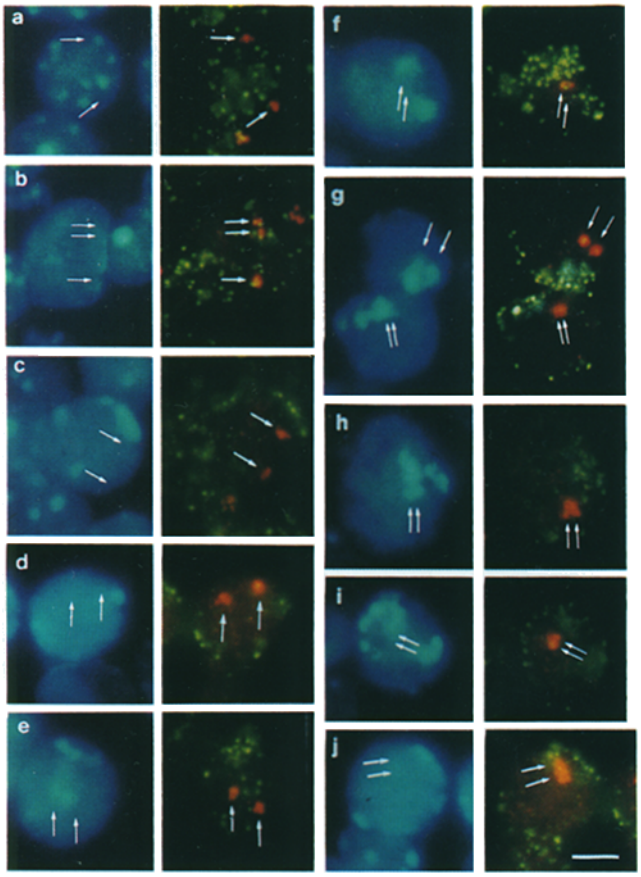

Figure 5. Sequential telomere clustering and homologous chromosome pairing during mouse meiotic prophase as revealed by two color FISH of chromosome-8–specific subsatellite (*red*) and telomere (*green*) DNA probes to testis tissue sections from mice at d 6 pp (*a* and *b*), 10 pp (*c–i*), and d 12 pp (*j*). DAPI counterstain is shown to the left of the FISH image. The position of the chromosome-8 signals is indicated by arrows in the FISH and the DAPI images. Note that in the latter images the position of the centromeres is indicated by the bright blue clusters of the major satellite DNA. In some images (e.g., *e*, *f*, and *h*) the telomere signals that appear distributed through the nuclear interior were recorded from focal plains at the lower or upper end of the respective nucleus. These signals were likely associated with the NE of the bottom or top nuclear region. (*a*) Prepuberal germ cell with separate (*arrows*) chromosome-8–specific signals (hereafter referred to as #8 signals); telomeres appear dispersed throughout the nucleus. (*b*) Mid-preleptotene nucleus showing separate #8 signals (*twin arrows* + *arrow*) and dispersed telomeres, while at this stage DAPI staining reveals no distinct signals for (peripheral) satellite DNA. One #8 signal appears as signal doublet (*twin arrows*). (*c* and *d*) Late-preleptotene nuclei showing assymetrically distributed and exclusively peripheral telomeres. Satellite DNA forms few, large DAPI bright clusters at the nuclear periphery; #8 signals separate. (*e*) Upper part of a late preleptotene nucleus. #8 signals separate. Most telomeres locate at the cluster site; some are still away from it. DAPI image shows two chromocenters in this focal plain. (*f*) Prominent telomere cluster at the upper end of a preleptotene/zygotene nucleus; centromeric satellite DNA forms two clusters (DAPI image). #8 repeats intimately aligned. (*g*) Two adjacent nuclei at preleptotene/zygotene exhibit tightly clustered telomeres. #8 signals appear aligned in the upper nucleus and paired in the lower nucleus. In the latter, few telomere signals are seen at the NE opposite to the cluster site. (*h*) Dispersion of clustered telomeres in a zygotene nucleus (bottom part of nucleus shown); #8 signals intimately paired. Two large satellite clusters are apparent in the DAPI image. (*i*) Zygotene nucleus with numerous satellite clusters dispersed along the NE (DAPI image) and #8 signals tightly paired. (*j*) Peripheral, asymmetrically distributed telomeres with paired #8 signals in a pachytene nucleus. Bar, 5 μm; conventional fluorescence microscopy.

Table II. Distribution of Satellite Clusters, Telomeres, and Chromosome 8 Subregional Probes in Meiotic Stems Cells and Spermatocytes of the Prepuberal Mouse Testis

Cell type	Detected at day x post partum	Satellite cluster distribution	Telomere signal distribution	Chromosome 8 repeats	Nuclei investigated
Prepuberal genocytes, A-type spermatogonia	4	Throughout nucleus	Throughout nucleus	Separate in 87%	50
Mid-preleptotene	6	Peripheral layer on NE	At NE and interior*	Separate in 94%‡	30
Late-preleptotone§	10	8 clusters at NE	Exclusively at NE	Separate in 100%	20
Early zygotene bouquet¶	10	Peripheral cluster at NE	Clustered at NE sector	Paired in 100%	6
Zygotene¶	10	2–10 peripheral clusters	At NE, partially clustered	Paired in 100%	50
Pachytene¶	12	5–10 peripheral clusters	Distributed over NE	Paired in 100%	100

*In 10% of these nuclei a subset of interior telomeres was seen in aggregation (compare Fig. 4 *b*).
‡23% of chromosome 8 signals were detected as doublets (see Fig. 5 *b*).
§Chromosome 8 repeat signals served as indicator for pairing. Occasional association of chromosome 8 signals in late-preleptotene nuclei could not be accounted for in this experiment. See Table III and triple labeling experiment in Fig. 7 for discrimination criteria.
¶The characteristic telomere and satellite DNA distribution and the histological context served as stage markers for zygotene and pachytene cells (see Fig. 3 and text for details).

chromosome-8 markers were separate, while satellite DNA (associated with proximal telomeres) formed 4–8 peripheral clusters (n = 20) (Fig. 5, *c-h*). Closely aligned or fused chromosome-8 signals indicated the onset of chromosome pairing in nuclei (n = 6) with tightly clustered telomeres (Fig. 5 *g*; Table II). In these nuclei centromeric satellite DNA formed a large chromocenter. 5 out of 32 tubuli investigated contained 2–5 cells that exhibited a full bouquet stage.

Post-bouquet zygotene and pachytene nuclei exhibited tightly paired chromosome-8 signals and exclusively peripheral telomeres (Table II). Groups of telomeres were seen in dispersion from the cluster site along the NE, while the huge chromocenter, seen at tightest telomere clustering was split up (Fig. 5, *i*, and *j*). In pachytene spermatocytes CLSM analysis (not shown) revealed the presence of 5–10 peripheral satellite clusters (n = 30), while telomeres remained attached to the NE (see Fig. 5 *j*, also 9 *d*). Exclusively peripheral telomeres have also been shown by serial section EM of mouse zygotene and pachytene nuclei (Glamann, 1986). Although neighboring prophase cells are part of a symplast that is believed to pass through spermatogenesis synchronously (e.g., Dym and Fawcett, 1971), these showed different degrees of telomere clustering (Fig. 5 *g*). This finding suggests bouquet formation to be a rapid, transient motif of the pairing process.

Tight Telomere Clustering Coincides with Axial Element Formation and Synapsis Initiation

To study further the relation of telomere movements to the onset of synapsis immunostaining of axial element proteins (AEPs) and transverse filament proteins (TFPs) was combined with telomere FISH in nuclei from paraffin testis sections of mice at d 10 and 12 pp. Mouse AEPs were immunostained using a polyclonal antiserum to 30 + 33–kD proteins of rat axial elements (Lammers et al., 1994). In rat meiocytes AEPs can be detected from leptotene/zygotene on up to diplotene (Offenberg et al., 1991). Within early-prophase oocytes they appear in large aggregates that often persist throughout prophase (Dietrich et al., 1992). In the mouse we made the following observations: spermatogonia and mid-preleptotene spermatocytes (Fig. 6 *a*) as well as Sertoli cells (not shown) were negative for immunostaining. Few large aggregates of immunopositive material of AEPs were first detected in late preleptotene cells (n = 37) as identified by exclusively peripherally distributed telomeres and few DAPI bright satellite DNA clusters (Fig. 6 *b–d*; Table III). When the cytoplasm was not completely removed, the surface of prophase nuclei was intensely stained by the AEP antibodies (e.g., Fig. 6, *b* and *f*).

Late-preleptotene nuclei (n = 10) exhibiting various degrees of clustered, peripheral telomeres showed interior antigen aggregates (Fig. 6 *b*), sometimes close to the cluster site (Fig. 6 *d*). In early-zygotene nuclei with telomeres in close association with each other (complete bouquet; n = 5), AEPs were seen in dispersion from the aggregates into the chromosomal chromatin, forming foci and short stretches of axial elements (Fig. 6 *e*). Nuclei exhibiting a more advanced formation of axial/lateral elements (zygotene, n = 5) showed two proximal telomere clusters, as identified by their association with DAPI bright chromocenters, remote from the cluster site (Fig. 6 *f*; compare also Fig. 8 *b* and *c*).

In zygotene nuclei post-bouquet (n = 50), some telomeres remained at the cluster site, while others were dispersed over the NE. AEP aggregates were no longer visible (Fig. 6 *f* and *g*; Table III). In few nuclei a subset of SCs was still aligned in parallel near the cluster site (Fig. 6 *g*). Pachytene nuclei (d 12 pp; n = 50) showed extensive synapsis with SCs, attached via their telomeres to the NE, meandering throughout the nuclear lumen (Fig. 6 *h*). In the vast majority of nuclei polarization of the prophase chromosomes was no longer apparent. Association of the centromeric satellite DNA led to the formation of a few, large and peripheral chromocenters (Fig. 6 *h*). These findings are in agreement with observations from serial sectioned mouse meiocytes (Glamann, 1986).

A triple labeling experiment was performed to reveal

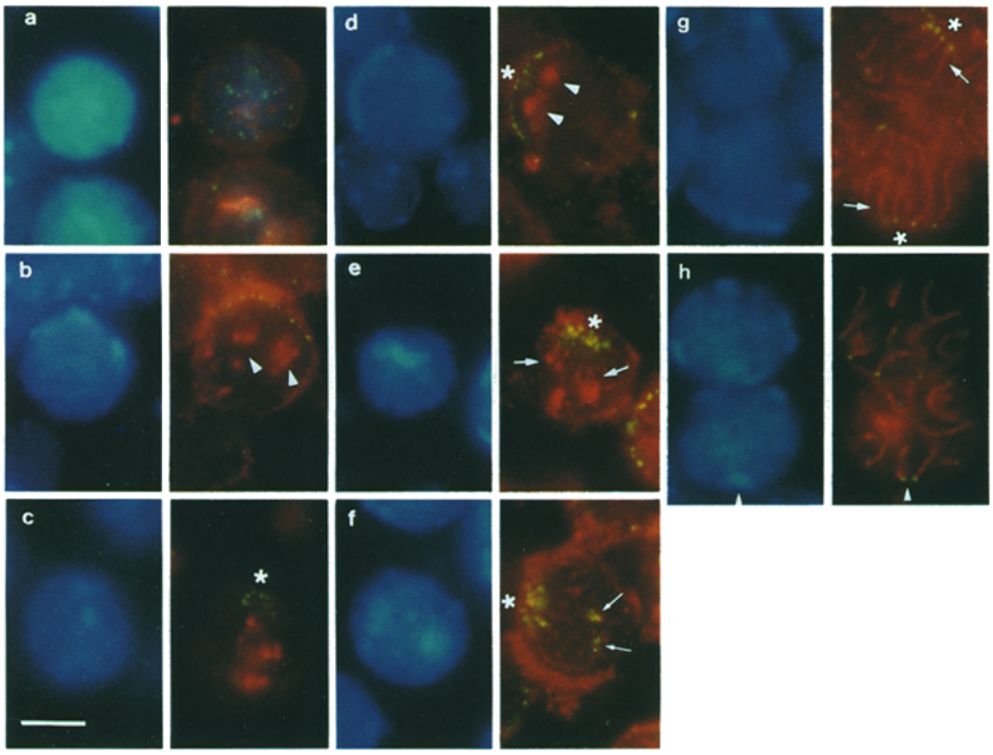

Figure 6. Telomere cluster formation and its relation to axial/lateral element (AE/LE) assembly, as revealed by simultaneous immunostaining of 30–33 kD AEPs (*red*) and telomere sequences by FISH (*green*) in prepuberal testis sections (day 10 and 12 pp). DAPI counterstain is shown to the left of the FISH image. (*a*) Prepuberal germ cell with dispersed telomeres, negative for immunostaining. (*b*) Late-preleptotene nucleus with peripheral telomeres and few, large AEP aggregates (*arrowheads*). (*c* and *d*) Late-preleptotene nuclei showing different motifs of clustered telomeres. The telomere cluster site is marked by an asterisk in *c–g*. (*c*) Top region of a late-preleptotene nucleus with partially clustered telomeres and few, large internal AEP aggregates. (*d*) AEP aggregates (*arrowheads*) concentrate near the telomere cluster site. (*e*) Early zygotene nucleus with tightly clustered telomeres and AEPs in a state of dispersion away from the large aggregates, as seen by foci and stretches of axial elements (*arrows*). (*f*) Two clusters of telomeres (*arrows*) are seen remote from the cluster site at the top of a bouquet nucleus. These telomere clusters represent proximal telomeres as seen by colocalization with DAPI bright chromocenters. (*g*) Two nuclei showing intense labeling of SCs, a fraction of which is still aligned in parallel near each cluster site (*arrows*). (*h*) Pachytene nucleus showing SCs meandering throughout the nuclear lumen. These are attached to the NE via their telomeres. Note the close proximity of two SC ends surrounded by DAPI bright satellite DNA (*arrowhead*). Bar, 5 μm; conventional fluorescence microscopy.

the position of AEPs, chromosome-8 repeats, and telomeres in the same bouquet cells. In such a cell peripheral telomeres concentrated at the cluster site, chromosome-8 signals were paired near a huge chromocenter, while immunostaining revealed foci and short stretches of AEPs (Fig. 7, *a–c*). Another nucleus revealed short stretches and foci of AEs/LEs, while chromosome-8 signals appeared tightly paired and telomeres and satellite DNA clusters

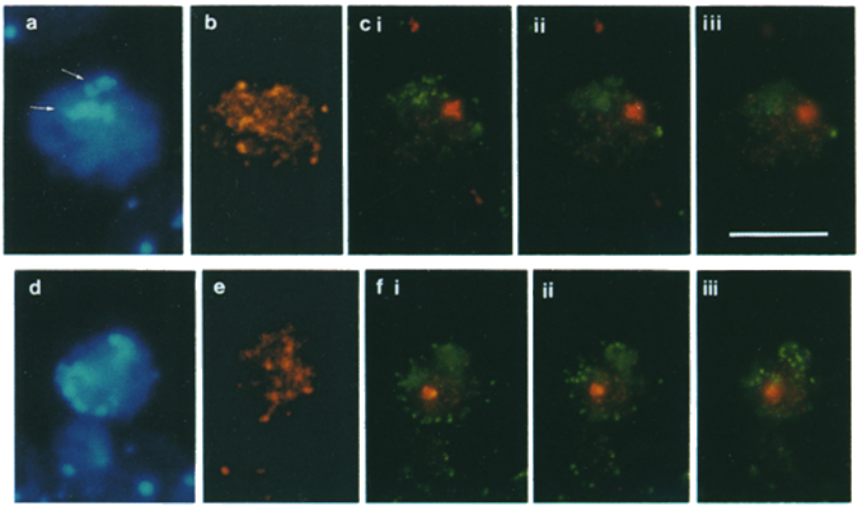

Figure 7. Immunostaining of AEPs (*reddish*) together with FISH of telomeres (*green*) and of chromosome-8–specific repeats (*red*). Two nuclei (*a–ciii* and *d–fiii*) from the same testis tubule show variable degrees of telomere cluster dissolution in consecutive focal plains. (*a*) DAPI-stained early zygotene nucleus (*blue*) showing two huge chromocenters formed by centromeric satellite DNA (*arrows*). (*b*) Same nucleus after anti-AEP immunostaining reveals short stretches and foci of AEPs. (*ci–iii*) Three consecutive focal plains spaced ~3 μm apart. (*ci*) Telomeres (*green*) are aggregated at the cluster site (lower part of nucleus), while chromosome-8 signals (*red*) appear elongated and paired. (*cii*) A single cluster of distal telomeres is seen away from the cluster site in section. (*ciii*) Top part of nucleus: no telomere signals in this focal plain. (*d*) DAPI image of an early zygotene nucleus showing satellite clusters dispersed across the NE. (*e*) AEP immunostaining reveals short stretches and foci of AEs. (*fi–iii*) Three consecutive focal plains of an early zygotene nucleus show dispersion of telomere signals (*green*) along the NE. Chromosome-8 signals (*red*) paired. (*fi*) Telomeres are peripheral and asymmetrically distributed in this focal plane. (*fii*) Most peripheral telomeres are asymmetrically distributed to left and top. (*fiii*) Focal plane showing upper nuclear region with some telomeres still clustered. Bar, 10 μm; conventional fluorescence microscopy.

Table III. Appearance of AEPs in Relation to the Distribution of Telomere FISH Signals and DAPI-stained Satellite Clusters

Cell type	Detected from day x pp on	Satellite cluster distribution	Telomere signal distribution	AEP immuno staining	Nuclei investigated
Mid-preleptotene	6	Peripheral layer on NE	In periphery and interior	Not detected*	30
Late-preleptotene	10	Few clusters at NE	At NE, partially clustered	AEP aggregates	37
Early-zygotene bouquet	10	Single, peripheral cluster at NE sector	At NE, clustered	AEP aggregates, and fragments of AEs and LEs	5
Zygotene	10	2–10 peripheral clusters	At NE, partially clustered	AEs and LEs	50
Pachytene	12	5–10 peripheral clusters	Distributed over NE	LEs	50

*Cells before late-preleptotene were negative for AEP immunostaining.

were distributed over a limited area of the NE (Fig. 7, *d–f*). These cells were identified as early zygotene by the absence of prominent AEP clusters and the presence of paired chromosome-8 signals.

Synapsis Initiates during the Bouquet Stage

TFPs (SCP1; Meuwissen et al., 1992) appear in synapsed regions of the SC (Offenberg et al., 1991). Their simultaneous detection in conjunction with telomere FISH was also performed to study telomere positions in relation to synapsis initiation. Before bouquet formation cells were negative for TFP immunostaining in our experiments (not shown). In few early zygotene nuclei with tightly clustered telomeres, TFPs were detected in small aggregates and short stretches of SCs (n = 4)(Fig. 8 *a*; Table IV). Few zygotene cells with prominent telomere clusters were observed (n = 4), which, like in previous experiments, exhibited two peripheral clusters of proximal SC ends relocated from the bouquet base (Fig. 8, *b–c*). Cells (n = 50) with intense SC immunostaining and asymmetrically distributed telomeres were also detected (Fig. 8 *d*). In pachytene nuclei telomeres were distributed over the NE (Fig. 8 *e*). In summary, these findings indicate that synapsis initiates during the time of telomere clustering, which has been observed in most organisms investigated (see Dernburg et al., 1995).

Centromere and Telomere Distribution in Spermatogenic Nuclei of the Adult Mouse Testis

The intranuclear distribution patterns of centromeric satellite DNA and telomeres established for the various cell types of the prepubertal mouse were observed in cells of the adult testis as well (Fig. 9, *a–d*). Spermatogonia with elliptical (A-type) and round nuclei (see above) exhibited numerous dispersed satellite DNA clusters and telomere signals throughout the nuclear lumen (Fig. 9, *a* and *d*). This resembles the distribution observed in prepuberal gonocytes. Spermatogonia (n = 25) from air-dried testis suspensions revealed 14–31 satellite clusters suggesting the association of centromeric heterochromatin. At a higher resolution, transmission electron microscopy in situ hybridization (TEM-ISH) showed some of the peripheral satellite clusters in intimate contact with the NE (Fig. 10 *b*) indicating association of these sequences with the nuclear lamina or nuclear envelope. A hybridization pattern exhibiting a Rabl orientation, i.e., adjacent satellite DNA clusters limited to the "Polfeld" and, on the opposite side of the nucleus, clustered distal telomeres representing the "Gegenpolfeld" (Rabl 1885), was only observed twice in the several hundreds of nuclei investigated (not shown). These nuclei most likely represented cells with polarized anaphase chromosomes.

Within a subset of nuclei the typical mid-preleptotene FISH pattern was observed as well (Fig. 9 *b*). Such nuclei have previously been described within adult testis tubuli at stage VIII of the cycle of the seminiferous epithelium which corresponds to the onset of meiotic prophase (Oud and Reutlinger, 1981; Dietrich and de Boer, 1983). Zygotene nuclei that are also detected in late stage VIII tubuli (e.g., Oud and Reutlinger, 1981) exhibited exclusively peripheral telomeres and centromeric satellite DNA clusters. Full bouquet cells with telomeres clustered were observed at a low frequency among zygotene cells (2 out of 154) (Fig. 9 *c*). Pachytene spermatocytes showed centromeric satellite DNA in 5–10 large, peripheral satellite clusters (n = 50), while telomeres were dispersed exclusively over the NE (Fig. 9 *d*). At a higher resolution, TEM-ISH revealed telomere hybridization signals at proximal and distal ends of the SCs (Fig. 10 *c*). The signals located at the interface of the differentially electron dense chromatin and cytoplasm, i.e., the position of the NE, (Fig. 10, *c* and *d*) indicating an intimate association with it. Nuclear envelope–anchored proximal SC ends were often located in close vicinity to other proximal SC ends, such that the DNA loops of the heterochromatin formed a common chromocenter (Fig. 10 *d*). Strictly peripheral telomere distribution was also confirmed by CLSM (not shown) and is consistent with results from serial section EM of mouse zygotene and pachytene spermatocytes (Glamann, 1986).

Besides cells of the spermatogenic line, Sertoli cells, the supportive cell lineage of spermatogenic cells, are frequently encountered in testis tissue sections. Sertoli cells of the adult testis exhibit a strikingly unique nuclear topography (e.g., Brinkley et al., 1986), which may be linked to their transcriptional activity (Haaf et al., 1990). Telomere FISH showed proximal telomeres fused into a bright staining "telocenter" at the periphery of the nucleolus associated heterochromatin clusters (Fig. 9 *b*, *small arrow*).

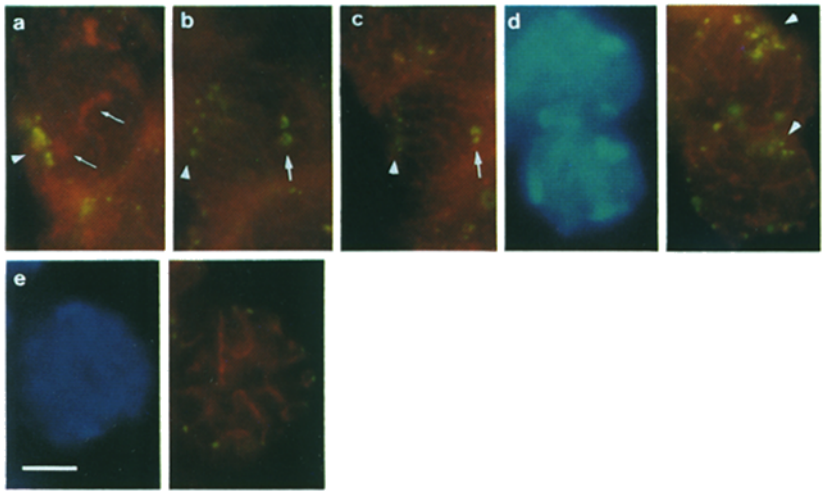

Figure 8. Telomere clusters in relation to synapsis initiation. Simultaneous immunostaining of 125 kD TFPs (*red*) and telomere sequences by FISH (*yellow*). DAPI images of nuclei shown in (*a–c*) were not informative. Thus, DAPI images are only shown for details *d* and *e* (left to the FISH image). (*a*) Early zygotene nucleus with tightly clustered telomeres (*arrowhead*). TFPs appear as aggregates (*arrows*) and stretches of SCs that indicate synapsis initiation. (*b* and *c*) Zygotene nuclei with two telomere groups (*arrows*) remote from the cluster site (*arrowhead*). Intense labeling of SCs indicates an advanced state of synapsis. (*d*) Pachytene nuclei showing extensive synapsis while telomeres appear partially clustered (*arrowheads*). (*e*) Pachytene nucleus displaying intensely stained SCs meandering through the nuclear lumen. Telomeres, at the ends of SCs, are seen exclusively at the nuclear periphery. Bar, 5 μm; conventional fluorescence microscopy.

Distal telomeres also appeared clustered (Fig. 9 *b*). TEM-ISH (not shown) confirmed this distribution.

Human Prophase Nuclei Exhibit Similar Motifs of Centromere and Telomere Distribution

To address the question whether the centromere and telomere behavior observed in mouse spermatogenesis harbors conserved motifs of the mammalian meiotic pairing process, human paraffin testis sections were also hybridized with telomere and human pancentromeric α–satellite (Mitchell et al., 1985) DNA probes (Fig. 11). Similar to the mouse, human spermatogonia exhibited numerous satellite and telomere signals distributed throughout the nucleoplasm (Fig. 11 *a*). Nuclei exhibiting centromeric α–satellite pressed against the nuclear envelope and showing interior and peripheral telomeres were detected as well (Fig. 11, *b* and *c*). This centromere/telomere topology corresponds to the one of mouse mid-preleptotene meiocytes. Nuclei exhibiting a chromosomal bouquet (Fig. 11, *d* and *e*) showed clustered peripheral telomeres, while most centromeres were seen in the nuclear interior (Fig. 11, *e–f*). This distribution is in accordance with observations made by serial sectioning (Rasmussen and Holm, 1978), but contrasts with the mouse bouquet stage where aggregation of proximal telomeres leads to the formation of a peripheral chromocenter (see above). Human meiocyte nuclei with exclusively peripheral telomeres (leptotene-pachytene;

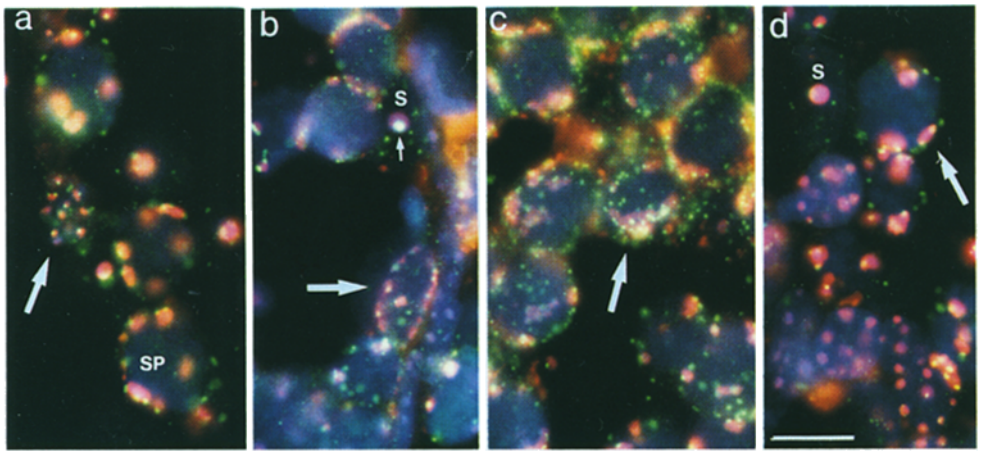

Figure 9. Distribution of centromeric satellite DNA (*red*) and telomere DNA sequences (*green*) in section nuclei of the adult mouse testis. The cells were identified by the histological context and FISH patterns based on their sequential appearance in the prepuberal testis (see Results; Fig. 3 *A*). (*a*) A-type spermatogonium (*arrow*) showing numerous satellite clusters and telomeres distributed throughout the nucleus. *SP*, Pachytene spermatocyte I exhibiting few peripheral telomeres and heterochromatin blocks. (*b*) Mid-preleptotene nucleus (*arrow*) showing centromeric satellite DNA compressed against the NE. Telomeres are seen within the nuclear lumen and at the NE. *S*, Sertoli cell displaying a prominent round satellite chromocenter and an associated telocenter (*yellow, small arrow*). Few distal telomere clusters are seen within the nucleus. Due to its decondensed chromatin the nuclear counterstain was faint for this nucleus. (*c*) The focal plain at the top region of a zygotene nucleus (*arrow*) shows clustered satellite DNA and telomeres at the polar region of the nucleus (bouquet arrangement; the overlay of numerous green telomere and red satellite signals results in a bulk of yellow signals). (*d*) Pachytene nucleus (*arrow*) showing distinctly peripheral localization of telomeres and satellite clusters. *S*, Sertoli cell. Several round spermatogonia exhibit numerous dispersed satellite and telomere signals. The faint blue counterstain in the nuclei results from double exposures of the DAPI counterstain on the red and green double band pass images. Bar, 10 μm; conventional fluorescence microscopy.

Table IV. Appearance of TFPs of the SC with Respect to Telomere FISH Signal Distribution

Cell type	Detected at day x pp	Telomere signal distribution	TFPs	Nuclei investigated
Early-zygotene bouquet	10	Clustered at NE sector	Aggregates and fragments of SCs	4
Zygotene	10	At NE, partially clustered	Fragments and complete SCs	40
Pachytene	12	Distributed over NE	Complete SCs	40

Cells before full bouquet formation were negative for TFP immunostaining in our assay.

see Rasmussen and Holm, 1978) showed most centromeres in the interior (Fig. 11, *g–h*). Human Sertoli cell nuclei, like those of the adult mouse, exhibited a unique nuclear morphology. A large nucleolus was capped by satellite DNA, while smaller satellite clusters and telomeres were seen throughout the nucleoplasm (Fig. 11 *j*).

Discussion

This investigation provides a detailed analysis on the chromosome as well as centromere and telomere distribution in premeiotic and meiotic cells of mouse and man. In both species homologues were variably arranged and separate in the vast majority of meiotic stem cells (spermatogonia) investigated. These findings are consistent with the absence of premeiotic association of homologous telomeres in human leptotene spermatocytes (Rasmussen and Holm, 1978), sex chromosomes at leptotene (Armstrong et al., 1994), X homologues at leptotene in human oocytes (Cheng and Gartler, 1994), and of Y homologues in human XYY prepuberal gonocytes (Ragg et al., 1995). In the mouse, alignment and pairing of homologous chromo-

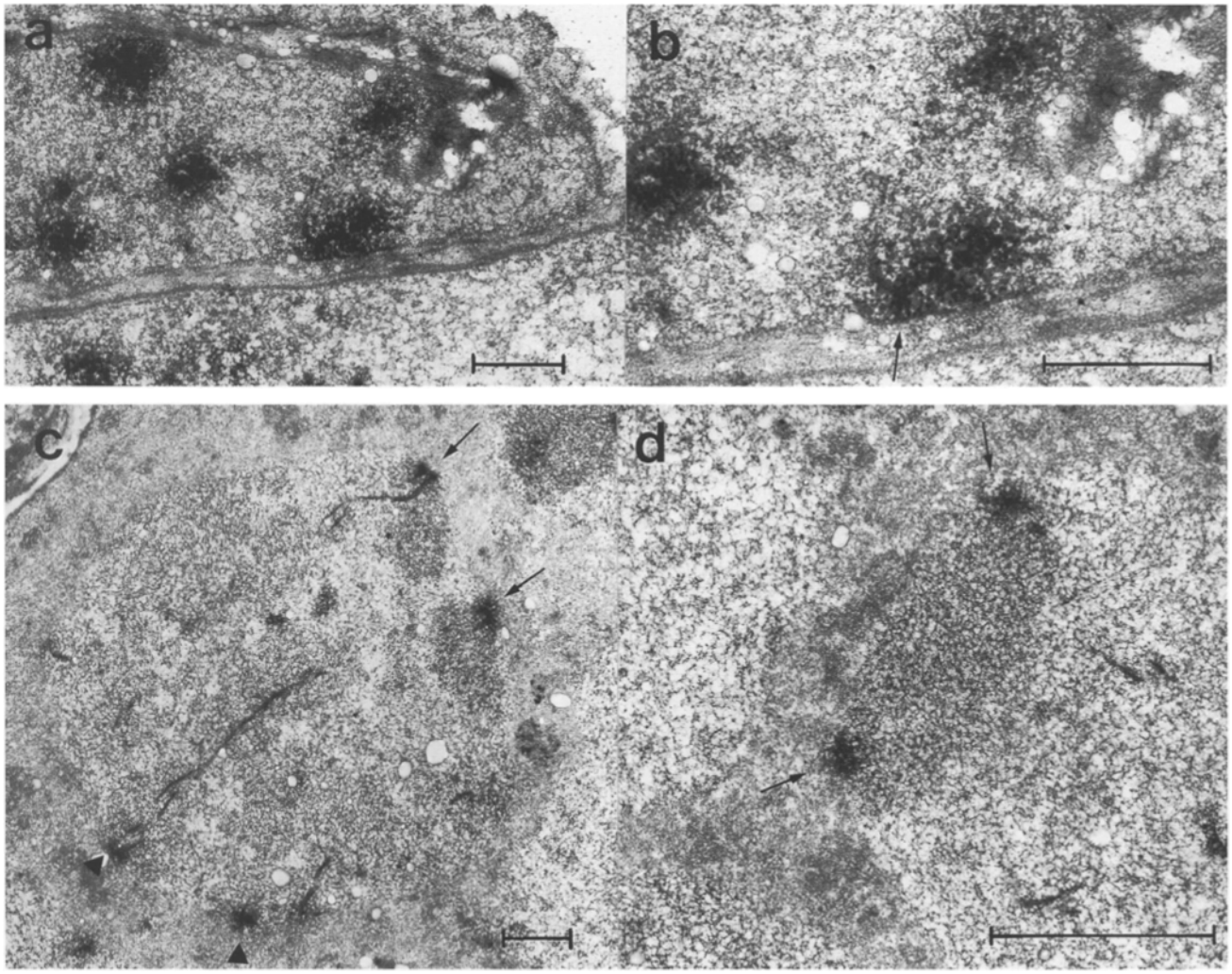

Figure 10. Electron micrographs of paraffin testis section nuclei after TEM-ISH with major satellite DNA (*a* and *b*), and telomere repeat probes (*c–f*). Black, electron-dense DAB precipitate is detected at the site of hybridization. (*a*) Spermatogonium shows densely labeled major sat DNA clusters within and at the periphery of the nucleus. Bar, 0.5 μm. (*b*) Detail of *a* showing satellite DNA staining the nuclear envelope (*arrow*). Bar, 1 μm. (*c*) Spermatocyte I nucleus hybridized with the telomere repeat probe. The attachment plaques of the SCs at the nuclear membrane (*arrows*, proximal telomeres; *Arrowheads*, distal telomeres) are labeled by DAB precipitate. Bar, 1 μm. (*d*) Detail of proximal telomere attachments (as identified by their associated heterochromatin) shows hybridization signals at the interface of the differentially electron dense cytoplasm and nuclear chromatin (i.e., the position of the NE). Bar, 0.5 μm.

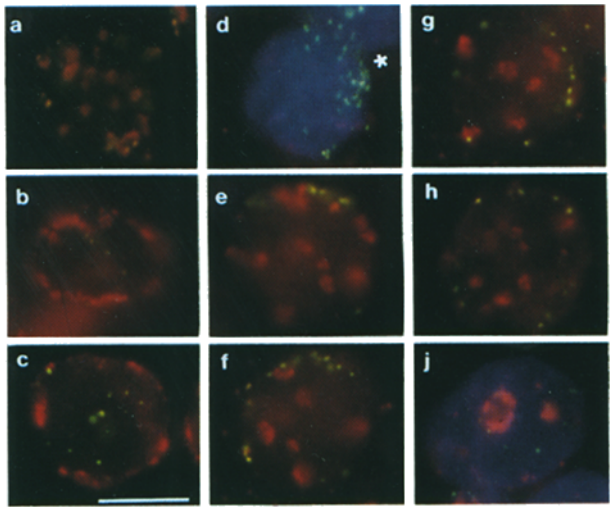

Figure 11. Meiocytes from human testis sections hybridized with pericentromeric alpha-satellite DNA (*red*) and telomere sequence probes (*yellow*). (*a*) A spermatogonium shows numerous satellite and telomere signals distributed throughout the nucleus (note: telomere signals appear weak and yellowish due to superexposure to the red satellite signals. Viewed with a specific FITC filter these appeared distinct [not shown]). (*b* and *c*) Early-prophase nuclei exhibit centromeric satellite DNA compressed against the NE, while telomere signals are seen within the nuclear lumen. (*d*) Prophase nucleus showing clustered telomeres (bouquet arrangement, *asterisk*). (*e*) Nucleus showing clustered telomeres at the nuclear periphery (top of nucleus). Note that centromeres are remote from the NE. (*f*) Nucleus showing partially clustered telomeres at the NE. (*g*) Asymmetrical distribution of peripheral telomeres and interior centromeres. (*h*) Pachytene nucleus with telomeres distributed over the NE and interior centromeres. (*j*) Human Sertoli cell nucleus. The satellite DNA cups a central nucleolus while smaller satellite clusters and telomeres are seen within the nucleus. In *d* and *e* the blue, DAPI counterstain was superimposed to the hybridization signals to better reveal the outline of the nuclei. Conventional fluorescence microscopy.

some-8 regions were associated with the formation of a chromosomal bouquet at the preleptotene/zygotene transition. Bouquet formation was preceded by a drastic, consecutive redistribution of centromeres and telomeres (Figs. 3 and 6), which did not profit from an apparent Rabl orientation of early meiotic chromosomes. Still, a Rabl orientation detected in some plant species (see Fussell, 1987) and tupaia somatic cells (Haaf and Ward, 1995) may facilitate bouquet formation at earliest meiotic prophase.

It has been suggested that the chromosome pairing process in mouse spermatogenesis initiates after premeiotic DNA replication (Guitart et al., 1985). This view is corroborated by our observation that the repetitive and presumably late replicating target DNA illuminated with the mouse chromosome-8–specific probe revealed signal doublets in a subset of mid-preleptotene nuclei (Fig. 5 *b*), a hybridization pattern that is indicative for replicated target DNA (Selig et al., 1992). It has been calculated that the time from premeiotic DNA replication to the onset of zygotene in the male mouse is only ~6 h or less (Oud and Reutlinger, 1981). According to this timing, the pairing process has to be very rapid and efficient.

The FISH patterns observed with the chromosome-8–specific probe at mid-preleptotene seem also to indicate that separate sister chromatids after DNA replication soon get tightly joined by a meiosis-specific factor other than catenation or incomplete replication (see Miyazaki and Orr-Weaver, 1994; Maguire, 1995). This is reflected by the absence of signal doublets from late preleptotene on. As the illuminated target region represents a repetitive DNA (Boyle and Ward, 1992) and the state of local chromatin conformation may be sensitive to technical variation, e.g., in the denaturation step, further studies are required to clarify this issue.

Centromere Movements to the Nuclear Envelope Precede Telomere Movements

According to the in situ analysis of prepuberal mouse testis cells the first detectable event at the chromosomal level of the meiotic pairing process is the transition of the centromeres to the NE during mid-preleptotene (Table II). Due to their physical proximity in the exclusively acrocentric mouse chromosomes, proximal telomeres follow these movements, while distal telomeres still locate in the nuclear interior and move somewhat later to the NE. Intranuclear association of distal telomeres detected in a subset of mid-preleptotene nuclei (Fig. 4 *b*) could be involved in orienting homologous chromosome territories (arms) before their transition to the NE.

A centromere and telomere distribution corresponding to the mouse mid-preleptotene topology was also detected in a subset of human spermatogenetic nuclei (Fig. 11, *b* and *c*). This topology represents a conserved motif of the mammalian pairing process. In human meiocytes with peripheral telomeres most centromeres were remote from the NE. This distribution contrasts with the exclusively peripheral centromeric satellite cluster distribution in mouse zygotene and pachytene nuclei. This discrepancy most likely reflects the predominantly submetacentric chromosome morphology in the human karyotype and suggests that peripheral satellite clustering during mouse meiotic prophase (Hsu et al., 1971; this report) is a secondary effect brought about by telomere movements (Fig. 3 *B*).

It can be assumed that the sequential transition of centromeres and telomeres to the NE (e.g., Figs. 2 and 6) requires the interaction of these chromosomal domains with some component of the nuclear matrix. TEM-ISH analysis suggests that attachment of telomeres to the inner nuclear membrane may involve telomeric $(TTAGGG)_n$ sequences (Fig. 10, *c* and *d*). In spread pachytene bivalents these locate at the ends of the SC cores (Moens and Pearlman, 1990) and exhibit a unique loop size (Heng et al., 1996). In human somatic nuclei it has been shown that terminal telomere sequences copurify with the nuclear matrix fraction (de Lange, 1992). At preleptotene telomere/nuclear matrix interactions could be used to move telomeres along the surface of chromosome territories to the NE (see model below).

Centromere and Telomere Movements Represent Conserved Motifs of the Pairing Process

The observed movements of meiotic centromeres and telomeres are distinct from the ones observed during the mi-

totic cell cycle of mouse (Vourc'h et al., 1993) and human cells (Ferguson and Ward, 1992, Weimer et al., 1992, Hulsplas et al., 1994). Premeiotic (spermatogonia) and Leydig cells exibit a centromere/telomere distribution similar to somatic cells such as mouse lymphocyte nuclei (Vourc'h et al., 1993). Sertoli cells, in contrast, display a unique type of centromere and telomere clustering, that is possibly related to their high transcriptional activity (Haaf et al., 1990).

Transient centromere and telomere movements during mouse and human meiosis, in principle, seem to parallel motifs of the pairing process recently established for the zygotic and asynaptic meiosis of the fission yeast *S. pombe*. In *S. pombe*, prophase telomere clustering is established at the onset of meiotic prophase and maintained throughout the entire meiotic prophase (Chigashige et al., 1994; Scherthan et al., 1994). The observations so far compiled in most, if not all, synaptic organisms suggest that telomere clustering represents a transient step during leptotene/zygotene (von Wettstein et al., 1984; Dernburg et al., 1995). The duration of chromosome polarization, however, may differ considerably between organisms (e.g., Bélár, 1928; Scherthan, 1995).

In mouse testis sections the number of fully polarized nuclei observed at the late-preleptotene/zygotene transition was <1%, and ~0.5% at pachytene in air dried preparations of mouse ovaries (Speed, 1982). These findings, together with the observation that even meiocytes of a symplast exhibited variable degrees of telomere clustering, suggest full bouquet formation to be an extremely short, transitional stage. It can not be excluded, however, that a considerable fraction of meiocytes passes through meiotic prophase without reaching a full bouquet stage.

Meiotic Telomere Movements May Relate to Nuclear and Chromatin Motion

Exceedingly complicated and saltatory nuclear and chromatin movements have been observed during leptotene/zygotene in live rat and insect meiocytes (Rickards, 1975; Parvinnen and Söderström, 1976). These observations apparently reflect the movements of numerous chromosome ends and chromosomes toward the cluster site. It can be assumed that the concerted movements of groups of ends and/or movements of numerous individual ends toward the cluster site could induce rotations and movements of the entire nucleus with respect to the centrosome. The convergence of telomeres is consistent with the formation of a few chromocenters during bouquet formation. Little is known, however, about the mechanism(s) by which these forces are created. Both, cytoplasmic forces generated by a tubulin-dependent mechanism (e.g., Rickards, 1975; Salonen et al., 1982; Svoboda et al., 1995; for review see Loidl, 1990) and internal nuclear forces (for review see de Boni, 1994) may be involved. Filamentous transmembrane connections between telomere attachments at the inner nuclear membrane and spherical dense structures at the cytoplasmic nuclear membrane of human meiocytes (see Boiko, 1983) could be involved in linking telomere attachments to the converging rails of tubulin which have been observed to encase the mouse spermatocyte I nucleus (Cherry and Hsu, 1984).

Homologues Align before Synapsis Initiation

Combined immunostaining of axial element proteins and telomere FISH revealed intranuclear protein aggregates in late-preleptotene nuclei. Dispersion of AEPs from the protein aggregates into chromosomal chromatin was observed at tight telomere clustering (Fig. 6 *e*). Initiation of synapsis was also observed in fully polarized nuclei (Fig. 8 *a*). The low number of cells detected at this transitional stage suggests a rapid assembly of these proteins into stretches of SCs. This implies that during bouquet formation meiotic chromosomes must have adopted their elongated conformation before axial/lateral element assembly. Furthermore, a substantial number of chromosomes or chromosomal regions has to be prealigned, allowing for synapsis initiation at multiple points in the nucleus. This is consistent with observations from spread meiocytes of mouse (Guitart et al., 1985) and other organisms (e.g., Hasenkampf, 1984; Albini and Jones, 1987). Thus, it can be concluded that telomere movements toward the cluster site precede synapsis initiation and are most likely associated with a homologue search and prealignment process. Polarization of prophase chromosomes provides for a favorable topological (bent) conformation of meiotic chromosomes, that helps to reduce and resolve entanglements of chromosomes before synapsis initiation.

In a few mouse bouquet nuclei groups of proximal telomeres were relocated from the cluster site, where the majority of telomeres were still seen in association. Telomere movements that lead to telomere dispersion over the NE post-bouquet (e.g., Glamann, 1986) could be associated with the migration of centrioles (e.g., Hughes-Schrader, 1943; Moens, 1974) or condensational forces (Scherthan et al., 1992; Weiner and Kleckner, 1994). It is tempting to speculate that homologues that have faithfully prealigned at the cluster site are rapidly removed from this site once they have initiated stable interactions. This would reduce the expenditure on homologue search of the remaining ones, a hypothesis that is consistent with the asynchronous onset of synapsis (Rasmussen and Holm, 1978; Jones and Croft, 1986; Santos et al., 1993).

Polarization of Early Prophase Chromosomes May Contribute to Homologue Search

Chromosome 1 territories painted in human spermatogonia were often separate and similar in shape to territories seen in somatic cell types (Fig. 2 *a*). During meiotic prophase their shape transforms into the well-known, threadlike chromosomes. In the mouse, this transformation was documented by an increase of the signal diameter and a change in the morphology of the chromosome-8 repeat signals. The unique chromosomal architecture of elongated chromosomes in the polarized nucleus may facilitate the congregation and alignment of numerous chromosome ends within a limited region of the nucleus, thus increasing the efficacy of homologue search (see Scherthan, 1996).

Homologue Pairing: A Model

Unifying our observations with present knowledge of the pairing process a model can be suggested (Fig. 12). Ac-

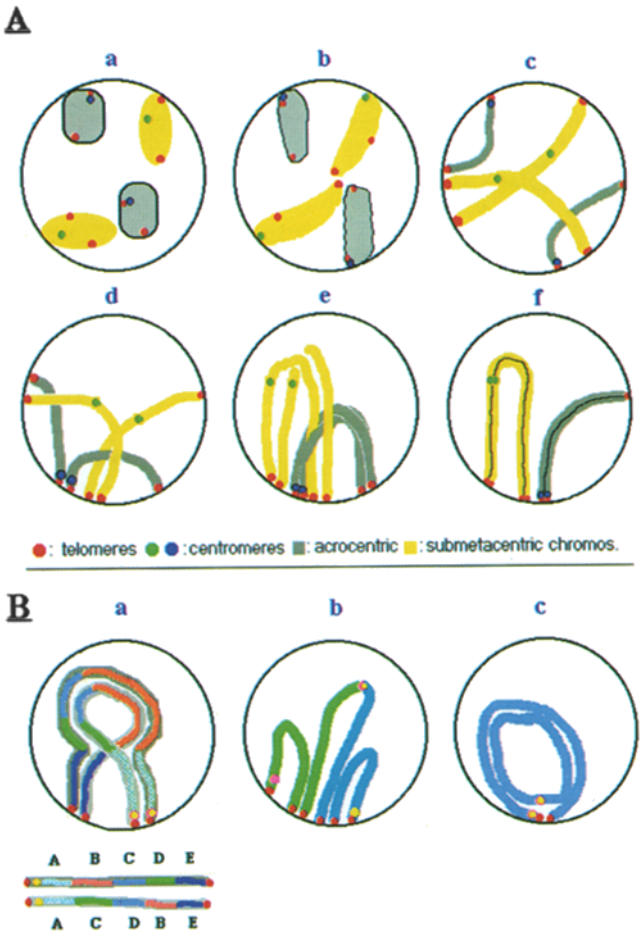

Figure 12. (*A*) A generalized, highly schematic model of the sequential movements of centromeres and telomeres and remodeling of chromosome territories during the pairing process. It is based on the observations made in this and earlier reports (see text). Telomeres (*red*) and centromeres (*green*) of a pair of submetacentric chromosome territories (*yellow*); centromeres (*blue*) of a pair of acrocentric chromosomes territories (*gray*). (*a*) In premeiotic cells chromosomes occupy compacted, often separate territories. Telomeres locate predominantly to the surface of territories (positions of centromeres and of territories arbitrary). (*b*) Mid-preleptotene: DNA replication is completed, all centromeres have moved to the NE, while telomeres lag behind (some of these associate in clusters within the nucleus). Chromosome territories start to elongate. (*c*) Telomeres have moved and attached to the NE, while chromosomes have adopted an elongated conformation (late-preleptotene, leptotene). Centromeres of metacentric chromosomes are remote from the NE, while centromeres of acrocentric chromosomes occupy a peripheral position. (*d*) Multiple encounters between elongated chromosomes contribute to homologue recognition. Presynaptic alignment is achieved during convergence of telomeres (e.g., late preleptotene/zygotene in mouse; leptotene/zygotene in human [Rassmusen and Holm, 1978], prezygotene in maize [Dawe et al., 1994]; prepachytene in mosquito [cf. Fig. 8 *a*; Wandall and Svendson, 1985]). (*e*) At tightest telomere clustering most chromosomes have aligned for a considerable fraction of their length, which still allows for resolution of entanglements of territories. (*f*) Presynaptic alignment is transformed into synaptic pairing. Ends of connected homologues (smaller ones probably first) are removed from the cluster site (e.g., gray chromosomes). (*B*) Alignment pairing of rearranged chromosomes with their normal homologues at the bouquet stage. (*a*) Inversion loop formation during bent-alignment in an inversion heterozygote. Long, colored oblongs and lettering demonstrate the orientation of the inverted segment in relation to the normal chromosome. (*b*) Robertsonian translocation heterozygote. Homologue recognition occurs near distal ends of bent aligned homologues. (*c*) Pairing of a ring chromosome with its normal homologue. Bent configuration of normal homologue facilitates homology search and pairing.

cording to this model premeiotic chromosomes occupy compacted, in most species, predominantly separate territories. Telomeres locate at the surface of these territories, and centromeric regions would also locate near the surface of territories (Fig. 12, *A*, *a*). The meiotic pairing process initiates after premeiotic DNA replication by transition of centromeres to the NE (Fig. 12, *A*, *b*), which ensures the NE contact of each chromosome territory. Telomeres, initially at the surface of territories, now move toward the inner nuclear membrane and attach to it. When telomeres have attached to the NE (e.g., late-preleptotene in the mouse), chromosome territories develop into long, thin cords with centromeres of submetacentric chromosomes remote from the NE (Fig. 12, *A*, *c*). Subsequently, telomere movements toward the cluster site produce numerous encounters among now elongated chromosomes, which contribute to homology testing at exposed pairing sites (Fig. 12, *A*, *d*). Convergence of chromosome ends increases the efficacy of homologue search and leads to prealignment of bent homologues (Fig. 12, *A*, *e*). These initiate stable interactions and relocate from the cluster site (Fig. 12, *A*, *f*). According to this view, breakage and reunion of lateral elements for interlock resolution during zygotene (von Wettstein et al., 1984) likely represent a mechanism for the removal of a few persistent interlocks.

The attractive features of the outlined model are that it can easily deal with highly variable chromosome distributions within the premeiotic nucleus and that it allows for the efficient pairing of rearranged chromosomes (Fig. 12 *B*). Inversion heterozygotes would lead to the formation of inversion loops, reciprocal translocation heterozygotes would form quadrivalents, and even a ring chromosome could efficiently pair with its intact partner (Fig. 12 *B*, *a–c*). The only prerequisite for the efficient pairing under these circumstances is that chromosomes maintain their bent configuration at the cluster site to allow for homology testing of aligned chromosomal segments. A simple 180° twist in one chromosome of, e.g., a pair of bent-aligned inversion heterozygotes, would facilitate inversion loop formation (Fig. 12, *B a*). When this spatial conformation is stabilized by crossovers, it will be seen as an inversion loop after spreading (e.g., Moses et al., 1984; Maguire and Riess, 1994). Alignment and pairing of rearranged chromosomes would require a surplus of chromosome maneuvers and thus more time for proper pairing. Accordingly, a rearranged chromosome and its normal homologue should show a strong tendency to be the last to pair. Prolonged prophase and impairment of spermatogenesis have been observed in mice with rearranged chromosomes (for review see de Boer and de Jong, 1989). However, efficient pairing of multiple Robertsonian translocation heterozygotes obviously facilitated by bent alignment has been observed (Johannisson and Winking, 1994). Chromosome

polarization, which has also been detected during prophase I in haploid rye (Santos et al., 1994), could be the underlying mechanism of foldback pairing (Gillies, 1974; Santos et al., 1994) and end associations (Loidl et al., 1991) frequently encountered in haploid meiosis. It may also mediate associations of nonhomologous chromosomes that have been observed to precede distributive disjunction (Loidl et al., 1994*b*).

We are grateful to Professor H. Zankl (University of Kaiserslautern) for continuous support; H. Fuge, E. Trelles, A. Regelin (University of Kaiserslautern) and P. de Boer (University of Wageningen), and two unidentified reviewers for stimulating comments on an earlier draft of the manuscript. We acknowledge the expert assistance of G. Schmidt in animal and tissue processing.

S. Weich received support from the Landesgraduiertenförderung Rheinland-Pfalz. This work was supported by the Deutsche Forschungsgemeinschaft (Sche 350/8-1) and in part by the Land Baden-Württemberg and European Community Biomet 2 grant BMH4-CT95-/139.

Received for publication 8 November 1995 and in revised form 4 June 1996.

References

Albini, S.M., and G.H. Jones. 1987. Synaptonemal complex spreading in *Allium cepa* and *A. fistulosum*. *Chromosoma (Berl.)*. 95:324–338.

Armstrong, S.J., A.J. Kirkham, and M.A.J. Hultén. 1994. XY chromosome behavior in the germ-line of the human male: a FISH analysis of spatial orientation, chromatin condensation and pairing. *Chromosome Res.* 2:445–452.

Ashley, T. 1994. Mammalian meiotic recombination: a reexamination. *Hum. Genet.* 94:587–593.

Bélár, K. 1928. Chromosomenreduktion. Die cytologischen grundlagen der vererbung. *In* Handbuch der Vererbungswissenschaft. E. Baur and M. Hartmann, editors. Gebrüder Borntraeger, Berlin. 1:168–201.

Bellvé, A.R., F.M. Clarke, Y.M. Bhatnagar, and D.A. O'Brian. 1977*a*. Dissociation of the mouse testis and characterization of isolated spermatogenic cells. *J. Histochem. Cytochem.* 25:480–494.

Bellvé, A.R., J.C. Caviccia, C.F. Millette, D.A. O'Brian, Y.M. Bhatnagar, and M. Dym. 1977*b*. Spermatogenic cells of the prepuberal mouse. *J. Cell Biol.* 74:68–85.

Blackburn, E.H. 1994. Telomeres: no end in sight. *Cell.* 77:621–623.

Boiko, M. 1983. Human meiosis VIII. Chromosome pairing and formation of the synaptonemal complex in oocytes. *Carlsberg Res. Commun.* 48:457–483.

Boyle, A.L., and D.C. Ward. 1992. Isolation and initial characterization of a large repeat sequence element specific to mouse chromosome-8. *Genomics.* 12:517–525.

Brinkley, B.R., S.L. Brenner, J.M. Hall, A. Tousson, R.D. Balczon, and M.M. Valdivia. 1986. Arrangements of kinetochores in mouse cells during meiosis and spermatogenesis. *Chromosoma (Berl.)*. 94:309–317.

Cheng, E.Y., and S.M. Gartler. 1994. A fluorescent in situ hybridization analysis of X chromosome pairing in human female meiosis. *Hum. Genet.* 94: 389–394.

Cherry, L.M., and T.C. Hsu. 1984. Antitubulin immunofluorescence studies of spermatogenesis in the mouse. *Chromosoma (Berl.)*. 90:265–274.

Chigashige, Y., D.Q. Ding, H. Funabiki, T. Haraguchi, S. Mashiko, M. Yanagida, and Y. Hiraoka. 1994. Telomere-led premeiotic chromosome movement in fission yeast. *Science (Wash. DC)*. 264:270–273.

Collins, C., W.L. Kuo, R. Segraves, D. Pinkel, J. Fuscoe, and J.W. Gray. 1991. Construction and characterization of plasmid libraries enriched in sequences from single human chromosomes. *Genomics.* 11:997–1006.

Cooke, H.J., and J. Hindley. 1979. Cloning of human satellite III DNA: different components are on different chromosomes. *Nucleic Acids Res.* 6:3177–3196.

Dawe, K.R., J.W. Sedat, D.A. Agard, and Z.W. Cande. 1994. Meiotic chromosome pairing in maize is associated with a novel chromatin organization. *Cell.* 76:901–912.

de Boer, P., and J.H. de Jong. 1989. Chromosome pairing and fertility in mice. *In* Fertility and Chromosome Pairing: Recent Studies in Plants and Animals. C.B. Gillies, editor. CRC Press, Boca Raton, FL. 37–76.

de Boni, U. 1994. The interphase nucleus as a dynamic structure. *Int. Rev. Cytol.* 150:149–171.

de Lange, T. 1992. Human telomeres are attached to the nuclear matrix. *EMBO (Eur. Mol. Biol. Organ.) J.* 11:717–724.

de Rooij, D.G. 1988. Regulation of the proliferation of spermatogonial stem cells. *J. Cell Sci. Suppl.* 10:181–194.

Dernburg, A.F., J.W. Sedat, W.Z. Cande, and H.W. Bass. 1995. The cytology of telomeres. *In* Telomeres. E.H. Blackburn and C.W. Greider, editors. Cold Spring Harbor Monograph Series, Cold Spring Harbor, NY. 295–338.

Dietrich, A.J.J., and P. de Boer. 1983. A sequential analysis of the development of the synaptonemal complex in spermatocytes of the mouse by electron microscopy using hydroxyurea and agar filtration. *Genetica (Dordrecht).* 61: 119–129.

Dietrich, A.J.J., E. Kok, H.H. Offenberg, C. Heyting, P. de Boer, and A.C.G. Vink. 1992. The sequential appearance of the synaptonemal complex during meiosis of the female rat. *Genome.* 35:492–497.

Dym, M., and D.W. Fawcett. 1971. Further observations on the number of spermatogonia, spermatocytes, and spermatids connected by intercellular bridges in the mammalian testis. *Biol. Reprod.* 4:195–215.

Ferguson, M.L.F., and D.C. Ward. 1992. Cell cycle dependent chromosomal movement in pre-mitotic human T-lymphocyte nuclei. *Chromosoma (Berl.)*. 101:557–565.

Fussell, C.P. 1987. The rabl orientation: a prelude to synapsis. *In* Meiosis. P.B. Moens, editor. Academic Press, Orlando, FL. 275–299

Gillies, C.B. 1974. The nature and extent of synaptonemal complex formation in haploid barley. *Chromosoma. (Berl.)*. 48:441–453.

Gilson, E.T., T. Laroche, and S.M. Gasser. 1993. Telomeres and the functional architecture of the nucleus. *Trends Cell Biol.* 3:128–134.

Giroux, C. 1988. Chromosome synapsis and meioti recombination. *In* Genetic Recombination. R. Kucherlapati and G.R. Smith, editors. American Society of Microbiology,Washington D.C. 497–527.

Glamann, J. 1986. Crossing over in the male mouse as analysed by recombination nodules and bars. *Carlsberg Res. Commun.* 51:143–162.

Goetz, P., A.C. Chandley, and R.M. Speed. 1984. Morphological and temporal sequence of meiotic prophase develpoment at puberty in the male mouse. *J. Cell Sci.* 65:249–263.

Guacci, V., E. Hogan, and D. Koshland. 1994. Chromosome condensation and sister chromatid pairing in budding yeast. *J. Cell Biol.* 125:517–530.

Guitart, M., M.D. Coll, M. Ponsa, and J. Egozcue. 1985. Sequential study of synaptonemal complexes in mouse spermatocytes by light and electron microscopy. *Genetica (Dordrecht).* 67:21–30.

Haaf, T., and D.C. Ward. 1995. Rabl orientation of CENP-B box sequences in *Tupaia belangeri* fibroblasts. *Cytogenet. Cell Genet.* 70:258–262.

Haaf, T., C. Steinlein, and M. Schmid. 1990. Nucleolar transcriptional activity in mouse Sertoli cells is dependent on centromere arrangement. *Exp. Cell Res.* 191:157–160.

Hasekampf, C.A. 1984. Synaptonemal complex formation in pollen mother cells of tradescantia. *Chromosoma (Berl.)*. 90:275–284.

Hawley, R.S., and T. Arbel. 1993. Yeast genetics and the fall of the classical view of meiosis. *Cell.* 72:301–303.

Heng, H.H.Q., J.W. Chamberlain, X.-M. Shi, B. Spyropoulos, L.-C. Tsui, and P.B. Moens. 1996. Regulation of meiotic chromatin loop size by chromosomal position. *Proc. Nat. Acad. Sci. USA.* 93:2795–2800.

Heyting, C., R. Dettmers, A.J.J. Dietrich, E.J.W. Redeker, and A.C.G. Vink. 1988. The sequential appearance of the synaptonemal complex during meiosis of the female rat. *Chromosoma (Berl.)*. 96:325–332.

Hiraoka, Y., A.F. Dernburg, S.J. Parmerlee, M.C. Rykowski, D.A. Agard, and J.W. Sedat. 1993. The onset of homologous chromosome pairing during *Drosophila melanogaster* embryogenesis. *J. Cell Biol.* 120:591–600.

Hopman, A.H.N., E. van Hooren, Ch.A. van de Kaa, P.G.P. Vooijs, and F.C.S. Ramaekers. 1991. Detection of numerical chromosome aberrations using in situ hybridization in paraffin sections of routinely processed bladder cancers. *Modern Pathol.* 4:503–513.

Hulsplas, R., A.B. Houtsmuller, P.-J. Krijtenburg, J.g.J. Bauman, and N. Nanninga. 1994. The nuclear position of pericentromeric DNA of chromosome 11 appears to be random in G0 and non-random in G1 human lymphocytes. *Chromosoma (Berl.)*. 103:286–292.

Hsu, T.C., J.E.K Cooper, M.L. Mace, Jr., and B.R. Brinkley. 1971. Arrangement of centromeres in mouse cells. *Chromosoma (Berl.)*. 34:73–87.

Hughes-Schrader, S. 1943. Polarization, kinetochore movements and bivalent structure in the meiosis of male mantids. *Biol. Bull. Acad. Sci. USSR.* 85: 265–300.

Johannisson, R., and Winking, H. 1994. Synaptonemal complexes of chains and rings in mice heterozygous for multiple Robertsonian translocations. *Chromosome Res.* 2:137–145.

Jones, G.H., and J.A. Croft. 1986. Surface spreading of synaptonemal complexes in locust. II. Zygotene pairing behavior.*Chromosoma (Berl.)*. 93:489–495.

Kleckner, N., and B. Weiner. 1993. Potential advantages of unstable interactions for pairing in meiotic, somatic, and premeiotic cells. *Cold Spring Harbor Symp. Quant. Biol.* 58:553–565.

Kluin, P.M., and D.G. de Rooij. 1981. A comparison between the morphology and cell kinetics of gonocytes and adult type undifferentiated spermatogonia in the mouse. *Int. J. Androl.* 4:475–493.

Kohli, J. 1994. Telomeres lead chromosome movement. *Curr. Biol.* 4:724–727.

Lammers J.H.M. , H.H. Offenberg, M. van Aalderen, A.C.G. Vink, A.J.J. Dietrich, and C. Heyting. 1994. The gene encoding a major component of the lateral elements of synaptonemal complexes of the rat is related to X-linked lymphocyte-regulated genes. *Mol. Cell. Biol.* 14:1137–1146.

Loidl, J. 1990. The initiation of meiotic chromosome pairing: the cytological view. *Genome.* 33:759–778.

Loidl, J., K. Nairz, and F. Klein. 1991. Meiotic chromosome synapsis in haploid yeast. *Chromosoma (Berl.)*. 100:221–228.

Loidl, J., F. Klein, and H. Scherthan. 1994*a*. Homologous pairing is reduced but not abolished in asynaptic mutants of yeast. *J. Cell Biol.* 125:1191–1200.

Loidl J., H. Scherthan, and D.B. Kaback. 1994*b*. Physical association between

nonhomologous chromosomes precedes distributive disjunction in yeast. *Proc. Natl. Acad. Sci. USA.* 91:331–334.
Maguire, M.P. 1988. Interactive meiotic systems. *In* Chromosome structure and function. J.P. Gustavson editor. Plenum Press, New York. 605–615.
Maguire, M.P. 1995. Is the synaptonemal complex a disjunction machine. *J. Hered.* 86:330–340.
Maguire, M.P., and R.W. Riess. 1994. The relationship of homologous synapsis and crossing over in a Maize inversion. *Genetics.* 137:281–288.
Metz, C.W. 1916. Chromosome studies on the Diptera. II. The paired association of chromosomes in the Diptera, and its significance. *J. Exp. Zool.* 21:213–279.
Meuwissen, R.L.J., H.H. Offenberg, A.J.J. Dietrich, A. Riesewijk, M. van Iersel, and C. Heyting. 1992. A coiled-coil related protein specific for synapsed regions of meiotic prophase chromosomes. *EMBO (Eur. Mol. Biol. Organ.) J.* 11:5091–5100.
Miazaki, W., and T. Orr-Weaver. 1994. Sister chromatid cohesion in mitosis and meiosis. *Annu. Rev. Genet.* 28:167–187.
Mitchell, A.R., J.R. Gosden, and D.A. Miller. 1985. A cloned sequence, p82H, of the alphoid repeated DNA family found at the centromere of all human chromosomes. *Chromosoma (Berl.).* 92:369–377.
Moens, P.B. 1974. Quantitative electron microscopy of chromosome organization at meiotic prophase. *Cold Spring Harbor Symp. Quant. Biol.* 38:99–107.
Moens, P.B. 1994. Molecular perspectives of chromosome pairing at meiosis. *BioEssays.* 16:101–106.
Moens, P.B., and R.E. Pearlman. 1990. Telomere and centromere DNA are associated with the cores of meiotic prophase chromosomes. *Chromosoma (Berl.).* 100:8–14.
Moens, P.B., C. Heyting, A.J.J. Dietrich, W. van Raamsdonk, and Q. Chen. 1987. Synaptonemal complex antigen location and conservation. *J. Cell Biol.* 105:93–103.
Moses, M.J., M.E. Dresser, and P.A. Poorman. 1984. Composition and role of the synaptonemal complex. *Symp. Soc. Exp. Biol.* 38:245–270.
Moyzis, R.K., J.M. Buckingham, C.S. Cram, M. Dani, L.L. Deaven, D.J. Jones, J. Meyne, R.L. Ratcliff, and J.R. Wu. 1988. A highly concerved DNA sequence, (TTAGGG)n, present at the telomeres of human chromosomes. *Proc. Natl. Acad. Sci. USA.* 83:6622–6628.
Nag, D.K., H. Scherthan, B. Rockmill, J. Bhargava, and G.S. Roeder. 1995. Heteroduplex formation and homolog pairing in yeast meiotic mutants. *Genetics.* 141:75–86.
Oakberg, E.F. 1956. A description of spermatogenesis in the mouse and its use in analysis of the cycle of the seminiferous epithelium and germ cell renewal. *Am. J. Anat.* 99:391–413.
Offenberg, H., A.J.J. Dietrich, and C. Heyting. 1991. Tissue distribution of two major components of synaptonemal complex of the rat. *Chromosoma (Berl.).* 101:83–91.
Oud, J.L., and A.H.H. Reutlinger. 1981. Chromosome behavior during early meiotic prophase of mouse spermatocytes. *Chromosoma (Berl.).* 83:395–407.
Padmore, R., L. Cao, and N. Kleckner. 1991. Temporal comparison of recombination and synaptonemal complex formation during meiosis in *S. cerevisiae*. *Cell.* 66:1239–1256.
Pardue, M.L., and J.G. Gall. 1970. Chromosomal localization of mouse satellite DNA. *Science (Wash. DC).* 168:1356–1358.
Parvinen, M., and K.-O. Söderström. 1976. Chromosome rotation and formation of synapsis. *Nature (Lond.).* 260:534–535.
Rabl, C. 1885. Über zelltheilung. *Morphologisches Jahrbuch.* 10:214–330.
Ragg, S., M. Härle, and H. Scherthan. 1995. Analysis of sex chromosome distribution in the gondal tissue of a 42,X/47,XYY mosaic by fluorescence in situ hybridization. *Mod. Pathol.* 8:295–298.
Rasmussen, S.W., and P.B. Holm. 1978. Human meiosis II. Chromosome pairing and recombination nodules in human spermatocytes. *Carlsberg Res. Commun.* 43:275–327
Rasmussen S.W., and P.B. Holm. 1980. Mechanics of meiosis. *Hereditas.* 93: 187–216.
Rhoades, M.M. 1961. Meioses. *In* The Cell: Biochemistry, Physiology, and Morphology., Vol. 3. Meiosis and Mitosis. J. Brachet and A.E. Mirsky, editors. Academic Press, New York. 1–75.
Rickards, G.K. 1975. Prophase chromosome movements in living house cricket spermatocytes and their relation to prometaphase, anaphase and granule movements. *Chromosoma (Berl.).* 49:407–455.
Rickards, G.K. 1981. Chromosome movements within prophase nuclei. *In* Mitosis/Cytokinesis. A.M. Zimmerman and A. Forer, editors. Academic Press, New York. 103.
Roeder, G.S. 1990. Chromosome synapsis and genetic recombination: their roles in meiotic chromosome segregation. *Trends Genet.* 6:385–389.
Salonen, K., J. Paranko, and M. Parvinen. 1982. A colcemid sensitive mechanism involved in regulation of chromosome movements during meiotic pairing. *Chromosoma (Berl.).* 85:611–618.
Santos, J.L., A.L. del Cerro, and M. Diez. 1993. Spreading synaptonemal complexes from the grasshopper *Chorthippus jacobsi*: pachytene and zygotene observations. *Hereditas.* 118:235–241.
Santos, J.L., M.M. Jimenez, and M. Diez. 1994. Meiosis in haploid rye: extensive synapsis and low chiasma frequency. *Heredity.* 73:580–588.
Scherthan, H. 1995. Chromosome evolution in muntjac revealed by centromere, telomere and whole chromosome paint probes. *In* Kew Chromosome Conference IV. P.E. Brandham and M.D. Bennett, editors. Royal Botanic Gardens, Kew. 267–280.
Scherthan, H. 1996. Chromosome behavior in earliest meiotic prophase. *Chromosomes Today.* 12:In press.
Scherthan, H., and T. Cremer. 1994. Methodology of non isotopic in situ hybridization in embedded tissue sections. Methods *Mol. Genet.* 5:223–238.
Scherthan, H., J. Loidl, T. Schuster, and D. Schweizer. 1992. Meiotic chromosome condensation and pairing in *Saccharomyces cerevisiae* studied by chromosome painting. *Chromosoma (Berl.).* 101:590–595.
Scherthan, H., J. Bähler, and J. Kohli. 1994. Dynamics of chromosome organization and pairing during meiotic prophase of fission yeast. *J. Cell Biol.* 127: 273–285.
Schmekel, K., and B. Daneholt. 1995. The central region of the synaptonemal complex revealed in three dimensions. *Trends Cell Biol.* 5:239–242.
Selig, S., K. Okumura, D.C. Ward, and H. Cedar. 1992. Delineation of replication time zones by fluorescence in situ hybridization. *EMBO (Eur. Mol. Biol. Organ.) J.* 11:1217–1225.
Speed, R.M. 1982. Meiosis in the foetal mouse ovary. *Chromosoma (Berl.).* 85: 427–437.
Svoboda, A., J. Bähler, and J. Kohli. 1995. Microtubule-driven nuclear movements and linear elements as meiosis specific characteristics of the fission yeasts *Schizosaccharomyces versatilis* and *Schizosaccharomyces pombe*. *Chromosoma (Berl.).* 104:203–214.
Sym, M., and G.S. Roeder. 1994. Crossover interference is abolished in the absence of a synaptonemal complex protein. *Cell.* 79:283–292.
Therman, E., and G.E. Sarto. 1977. Premeiotic and early meiotic stages in the pollen mother cells of eremus and in human embrionic oocytes. *Hum. Genet.* 35:137–151.
Vergowen, R.P.F.A., S.G.P.M. Jacops, R. Huiskamp, J.A.G. Davids, and D.G. de Rooij. 1991. Proliferative activity of gonocytes, Sertoli cells and interstitial cells during testicular development in mice. *J. Reprod. Fert.* 93:233–243.
Vergowen, R.P.F.A., R. Huiskamp, R.J. Bas, H.L. Roepers-Gajadien, J.A.G. Davids, and D.G. de Rooij. 1993. Postnatal development of testicular cell populations in mice. *J. Reprod. Fert.* 99:233–243.
von Wettstein, D., S.W. Rasmussen, and P.B. Holm. 1984. The synaptonemal complex in genetic segregation. *Annu. Rev. Genet.* 18:331–413.
Vourc'h, C., D. Taruscio, A.L. Boyle, and D.C. Ward. 1993. Cell cycle–dependent distribution of telomeres, centromeres, and chromosome-specific subsatellite domains in the interphase nucleus of mouse lymphocytes. *Exp. Cell Res.* 205:142–151.
Wandall, A., and A. Svendsen. 1985. Transition from somatic to meiotic pairing and progressional changes of the synaptonemal complex. *Chromosoma (Berl.).* 92: 254–264.
Weimer, R., T. Haaf, M. Poot, and M. Schmid. 1992. Characterization of centromere arrangements and test for random distribution in G0, G1, S, G2, G1, and early S′ phase in human lymphocytes. *Hum. Genet.* 88:673–682.
Weiner, B., and N. Kleckner. 1994. Chromosome pairing via multiple interstitial interactions before and during meiosis in yeast. *Cell.* 77:977–991.
Zickler, D. 1977. Development of the synaptonemal complex and "recombination nodules" during the meiotic prophase in the seven bivalents of the fungus *Sordaria macrospora* Auersw. *Chromosoma (Berl.).* 61:289–316.